安徽建筑大学
ANHUI JIANZHU UNIVERSITY

英 文 翻 译

题　　目：多参数水质监测系统研制

姓　　名：夏庆生

学　　号：17205040229

学　　院：电子与信息工程学院

专　　业：通信工程

指导教师：徐荃

完成时间：2021 年 4 月 30 日

A MEMS-Based Multi-Parameter Integrated Chip and Its Portable System for Water Quality Detection

Abstract

As an important means to protect water resources, water quality detection is of great social and economic significance. Water quality detection sensors processed by micro-electro-mechanical system (MEMS) technology have the advantages of low-cost, small size, and high sensitivity. In this paper, a multi-parameter water quality detection integrated sensor chip is further studied, and a portable detection system using this chip is developed. Temperature, pH, oxidation-reduction potential (ORP), conductivity and concentration of copper ions (Cu^{2+}) are selected as typical water quality parameters. Experiments of sensor calibrations using this portable detection system were performed in standard solutions. The sensor has a sensitivity of −57.34 mV/pH in pH detection and 5.95 Ω/°C in temperature response. ORP is directly detected by Pt microelectrode on the chip and the relative error is less than 3%. The electrode constant of the sensor is 1.416 cm−1 and the linearity is 0.9995 in conductivity detection. With the gold nanoparticles deposited on the electrode, the detection peak of Cu^{2+} appears at 280 mV and the sensor shows good linearity to the concentration of Cu^{2+} in the range of 0–0.6 mg/L. The detection limit of Cu^{2+} concentration is 2.33 μg/L. Through measurement and calculation, the accuracy of the portable system is within 4%. This portable multi-parameter water quality detection system with the MEMS-based integrated chip shows great potential in the field and fast detection.

1. Introduction

The contamination of water has attracted many people's attention all over the world. Water protection can start from the water quality inspection through the detection of physical and chemical indicators in the water samples. It can obtain the status of water pollution and also provide an important reference for subsequent treatment decisions [1]. Due to the lack of rapid and effective detection and treatment methods, large-scale water pollution incidents are still occurring repeatedly [2,3]. In the past three decades, more and more researches focus on water quality detection and lots of guidelines and quality standards have been developed by specialized regulators and organizations [1,3]. Traditional water quality detection requires taking water samples back to the laboratory, which takes too much time. As computer and communication technologies increase, the development trend of water detection instruments is low-cost, miniaturization, easy operation, high precision and reliability [1,2,3].

A series of parameters can be used to characterize water quality, including pH, turbidity, free chlorine, dissolved oxygen, conductivity, temperature, oxidation-reduction potential (ORP), heavy metal, and so on [1,4]. The detection of a single parameter is not enough to judge water quality [2]. However, it is impractical to monitor all the parameters in water at the current stage because of the complexity of replacing, regulating and maintenance of the sensor probes [1]. Multi-parameter, integrated and simultaneous detections are the foci of current researches. The appearance and development of micro-sensors make the multi-parameter integrated detection become a reality [2,3,4,5,6,7]. The manufacture of these integrated sensor chips adopts advanced and mature processes such as thick-film technology [5], inkjet printing techniques [2,6] and micro-electro-mechanical system (MEMS) technology [4,8]. For remote and portable monitoring of water quality, Internet of Things technology [3], microcomputer technology [9,10] and wireless communication technology like Wi-Fi [3] and Bluetooth [9] are used frequently.

For the water quality, the temperature is an important factor in the determination of many physical and chemical parameters of water quality, and it can directly affect the measurement results of pH, conductivity and other monitoring items [1,2,5]. Apart from glass liquid thermometers and bimetal thermometers, thermistors are also commonly used. Among them, the resistance temperature detector (RTD) processed from platinum (Pt) is often used because of its good stability and accuracy [4]. As a measure of acidity and alkalinity of solutions, pH can reflect whether water quality is polluted by acid or alkaline substances and indicate the degree of pollution, which is very important to human health [11]. For a multi-parameter integrated sensor chip and its portable system, the traditional glass electrode of pH is not a suitable choice. In previous studies, metal oxide electrodes showed good Nernst response, of which RuOx had the characteristics of low contamination, easy preparation and good chemical resistance [12]. As one of the electrical and physical characteristics of water quality, conductivity reflects the level of electrolytes present in the water and acts as an important indicator of the purity of water [11,12].

ORP monitoring first appeared in the study of chlorine oxidation ability. Its value is related to the disinfectant efficiency of water quality [11]. Currently, ORP detection has been recognized by many international and national health standards. As a drinking water standard, ORP value takes into account varieties of chemical elements in the water, which is easy to display the water quality with electronic instruments. According to the Environmental Protection Agency (EPA), the ORP of drinking water should be approaching 250 mV [13]. ORP is an electrochemical parameter and the principle of an ORP electrode is not obscure. The direct way to measure it is to detect its potential against a reference electrode (RE) [11,14].

Heavy metal ions pollution has become a serious environmental problem. In aquatic ecosystems, heavy metals ions change the fine structure of the plant's locomotor, inhibit their photosynthesis and respiration, alter the composition of nucleic acids, and affect cell volume [15,16,17]. Excessive levels of heavy metals in animals cause inactivation of enzymes and cytotoxicity, which further affect genetic expression, damage nerve tissue and important immune organs [18,19,20]. The

traditional methods for heavy metal ions detection include but are not limited to atomic fluorescence spectrometry, inductively coupled plasma, atomic absorption spectrometry, ultraviolet-visible spectrophotometry [21,22], and electrochemical detection. The electrochemical detection is simple in principle and easy to implement just with a triple-electrode system. A triple-electrode system is composed of a working electrode (WE), a counter electrode (CE) and a RE. By using different materials to modify the working electrode, identification of specific ions can be achieved and detection performance can be improved [15]. For instance, the microelectrodes modified by gold nanoparticles (AuNPs) show satisfied analytical performances in the detection of copper, lead and zinc ions [23].

In this paper, a multi-parameter water quality detection integrated chip is further studied. The previous work about the design, fabrication, and testing results of the temperature, pH and conductivity sensors on this integrated chip has been reported [12]. This paper makes some additions. The new research focuses on the development of ORP and copper ions (Cu^{2+}) detection on the integrated sensor chip, and its portable detection system of the above five parameters is designed and developed. This multi-parameter integrated chip is fabricated by MEMS techniques and electrochemical modification technology. The Pt film electrode is prepared to detect the potential of ORP. The copper irons detection sensor adopts an interdigital electrodes structure, with an AuNPs film deposited on its surface to improve the detection capability. In our portable detection system, a piece of STM32F407VGT6 chip is used as the main microcontroller unit (MCU). A 0.96-inch organic light-emitting diode (OLED) screen is used to display data. A Bluetooth chip is connected to the serial port in the MCU, which can transmit data to the computer or other mobile devices to display the data and waveforms. This project aims to develop a portable water quality detection system based on the multi-parameter integrated sensor chip, which can be used to detect parameters including temperature, pH, conductivity, ORP and copper ions in water standards [24,25,26]. In the standards, the pH of drinking water should be between 6.5 and 8.5 at normal temperature [24,25].

The conductivity of general natural water is less than 1.5 mS/cm, while water containing inorganic salts can reach 10 mS/cm [26]. The concentration of copper ions in water should be less than 1 mg/L [24,25]. The experiments with the MEMS sensor chip and its portable system proposed in this project show satisfactory results in terms of miniaturization, accuracy, linearity, and sensitivity. The whole system has great potential for portable, rapid and accurate measurements of actual water samples.

2. Materials and Methods

2.1. Multi-Parameter Integrated Sensor Chip

Considering the good electrical and temperature characteristics, we chose Pt as the substrate metal of the multi-sensor integrated chip [12]. We used 4-inch silicon wafer processing technology and basic MEMS technology to fabricate the structure of each part of the microchip. The simplified fabrication process [12] is shown in Figure 1.

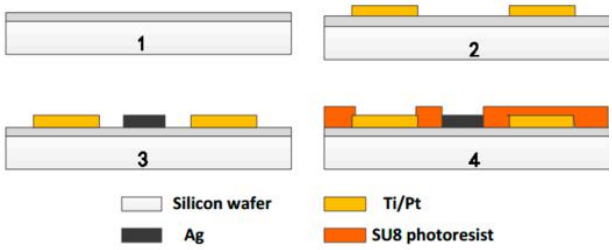

Figure 1. Fabrication process of the integrated microchip.

Before used, the silicon wafers were boiled in a concentrated H2SO4/H2O2 mixture and deionized water at 2000 °C for 20 min successively. Then, the wafers were sequentially put into acetone, alcohol, and deionized water for ultrasonic cleaning. Since silicon has electrical conductivity, it is necessary to perform an oxidation treatment on the silicon surface for insulation. The SiO_2 layer formed by thermal oxidation was 600–900 nm thick (Figure 1 Step 1). The surface of the SiO2 layer was then cleaned using plasma of oxygen. We used photolithography to make the required sensor shape patterns appear on the wafer. After being cleaned by oxygen plasma, metal Ti and Pt were sputtered on the position of the sensors on the surface of the wafer by magnetron sputtering technology (Figure 1 Step 2). The Ti performed as bonded metal to enhance the adhesion of Pt to the substrate. Excess metal and photoresist were removed with acetone by lift-off processes. Repeated the above steps to get a layer of metallic Ag for future use (Figure 1 Step 3). Then a photoresist insulating layer of SU8 was prepared around the sensor electrodes metal layer also by photolithography technology (Figure 1 Step 4). Subsequently, the silicon wafer was sliced to form a batch of single chips of 8 mm × 10 mm. The integrated

chip of multi-parameter water quality sensors is shown in Figure 2. Each chip was connected to the PCB board by golden wire ball welding finally.

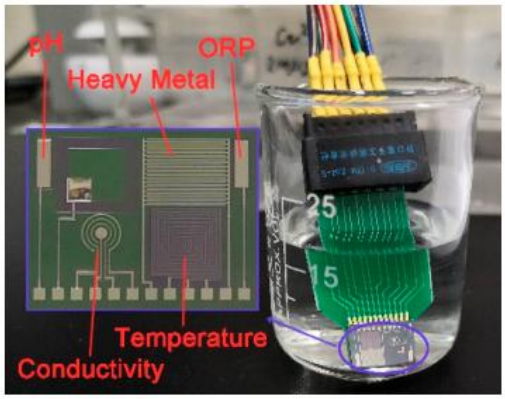

Figure 2. Multi-parameter integrated chip

The pH electrode and ORP electrode are rectangular in shape and 500 μm × 2000 μm in size. The basic principles of the two parameters are similar and both based on the potential detection of the Nernst equation as described in Equation (1).

$$E = E_0 + \frac{RT}{nF} \ln \frac{A_{ox}}{A_{red}} \quad (1)$$

where E is the potential generated on the surface of metal electrodes. E0 is the standard electrode potential (mV). R is the ideal gas constant (8.314 J·mol−1·K−1). F is the Faraday constant (96,485 C/mol). The symbol n represents the number of electron transfers in the reaction. Aox represents the activity of oxidizing substances (mol/L) and Ared represents the activity of the reducing substance (mol/L). Obviously, the potential E we need to measure is affected by the thermodynamic temperature T (K). The measuring electrode of the ORP sensor is an inert Pt electrode, which can play the role of electron transfer and does not participate in the reaction. Therefore, ORP is measured directly by detecting the potential of Pt microelectrode against an Ag/AgCl reference electrode as a single voltage in millivolts. The Pt measuring cell detects changes in ORP, while the RE provides a stable comparison signal.

RuOx is sensitive to the pH of the solutions. After deposited a RuOx layer on the surface of Pt microelectrode by cyclic voltammetry (CV) in RuCl3 solution, the RuOx/Pt electrode turns into a pH sensor combined with the Ag/AgCl reference

electrode. The simplified induction mechanism of RuOx [27] can be described by Equation (2). The Nernst equation of RuOx is reduced to Equation (3).

$$R_u{}^{IV}O_2 + e^- + H^+ = R_u{}^{III}O(OH) \quad (2)$$

$$E_{p^H} = E_0 - \frac{RT}{F} ln \frac{c(R_u{}^{III})}{c(R_u{}^{IV}) \cdot c(H^+)} \quad (3)$$

The c($R_u{}^{III}$) and c(R^{IV}) represent the activities of Ru(III) and Ru(IV), respectively. In the solid state, they are nearly equal. The c(H^+) is the concentration of H^+ and its negative logarithm is defined as pH. At 25 °C, it is approximately Equation (4).

$$E_{p^H} = E_0 + 0.05914 \times \lg c(H^+) \quad (4)$$

That means the theoretical slope is −59.14 mV/pH. The same as ORP, the pH sensing electrode measures the open circuit potential (OCP).

The conductivity sensor was designed as a four-electrode type. The advantage of the 4-electrode conductivity sensor lies in the fact that there is negligible current flowing through the inner electrodes where the measurement is made [12]. Conductivity is the inverse of resistivity. It is an electrical physical quantity, and its relationship with voltage and current can be described as Equation (5).

$$S = k \cdot G = k \cdot I/U \quad (5)$$

where S is the conductivity (mS/cm), k the electrode constant (cm^{-1}), G the conductance (mS), I the current (μA), and U the voltage (mV). The detection method is applying an AC stimulus to the sensor and measuring the voltage and current across it. Based on the experimentally measured voltage, current, and electrode constant, the electrical conductivity of the water quality can be calculated. Also, conductivity is affected by temperature as Equation (6).

$$S_t = S_{18}[\alpha(t - 18) + 1] \quad (6)$$

where St is the conductivity (mS/cm) at t °C and S18 means the conductivity (mS/cm) at 18 °C. The symbol α is the temperature coefficient (°C−1).

As stated previously, RTD is widely used to measure temperature. Its resistance-temperature characteristic can be expressed as Equation (7).

$$R_t = R_0 \cdot [1+\beta(t-t_0)] \quad (7)$$

where Rt means the resistance (Ω) at t °C and R0 means the resistance (Ω) at t0 °C. And β is the temperature coefficient ($℃^{-1}$) of the material. The method of measuring resistance is simple. The temperature sensor in this study is a Pt microband with an orthogonal structure. The connection adopts a three-terminal connection method [4,12].

For copper ions detection, an electrochemical 3-electrode system was built in this work. Two rows of interdigital electrodes were designed as WE and CE respectively. Each row of the electrodes consisted of 15 finger electrodes (3500 μm × 50 μm) with the interdigital spacing of 50 μm. A film of AuNPs was deposited on the surface of WE in 2 mM HAuCl4 solution by cyclic voltammetry. The deposition potential was −0.2 V and the deposition time was 300 s [23]. In this 3-electrode system, an Ag/AgCl electrode was used as RE.

2.2. Hardware System

The detection system consists of an integrated sensor chip as described above, a control module, a human-computer interaction module, analog-to-digital (A/D) conversion, and signal conditioning circuit. The hardware block diagram of the detection system is shown in Figure 3.

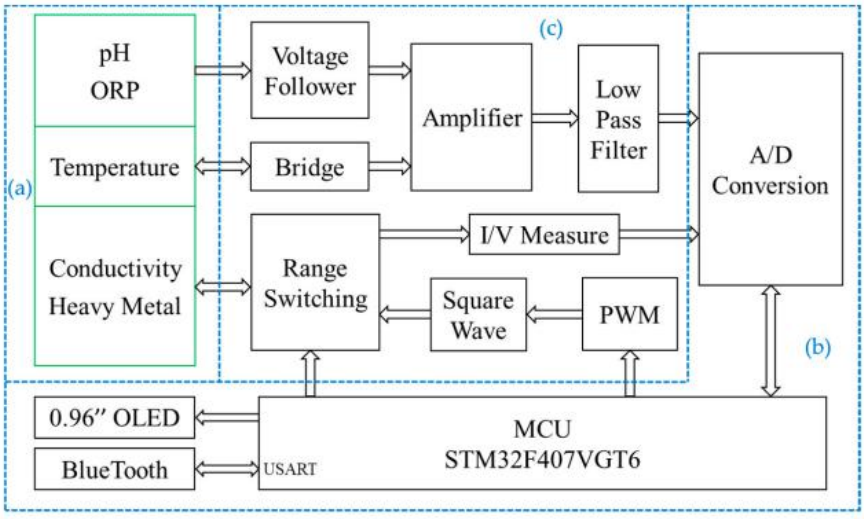

Figure 3. Hardware system block diagram: (a) integrated sensor chip; (b) control module, human-computer interaction module and A/D conversion (control board); (c) signal conditioning circuit (detection board).

The control module adopts a piece of STM32F407VGT6 chip (STMicroelectronics, Geneva, Switzerland) as the main controller and contains the smallest system composed of the external crystal oscillator, debugging interface, reset circuit and so on. The human-computer interaction module consists of a 0.96-inch OLED screen, a Bluetooth unit (BLE103 chip, Wenheng Technology, Shanghai, China) [28] and a serial communication port of USART. The OLED screen can display real-time data, which is used to prompt the running state of the system and display the measurement results directly. By using Bluetooth communication, we can connect the portable water quality detection system with a smartphone to achieve functional control, data transmission, and analysis. In order to store large amounts of data locally, we use the USART port to transmit data to the computer. Data processing and result curve drawing are performed by the Origin software (Version 9.6.5, OriginLab, Northampton, MA, USA). A low power analog-to-digital converter (ADC) chip AD7790 (Analog Devices, Norwood, MA, USA) is used in the measurement. Under the reference voltage of 2.5 V, it can obtain the smallest measurement of 0.0763 mV [29]. When the pH sensor acts as −59.14 mV/pH, the smallest theoretical change for pH we can detect is 0.0763/59.14 = 0.0013 pH. In the detection system, only two decimal places are retained to achieve a resolution of 0.01 pH.

The signal conditioning circuit mainly includes filters, operational amplifiers, and the signal generator circuit. For the OCP measurement of pH and ORP, an AD8279 chip (Analog Devices, Norwood, MA, USA) is used to amplify or reduce their voltage by two times. Then it adds the compensation voltage of 1.25 V to get the measurement voltage in 0–2.5 V. Considering impedance matching, two voltage followers are used. The signal conditioning circuit of pH and ORP is shown in Figure 4. The RE of them is connected to a zero potential of GND through a resistor.

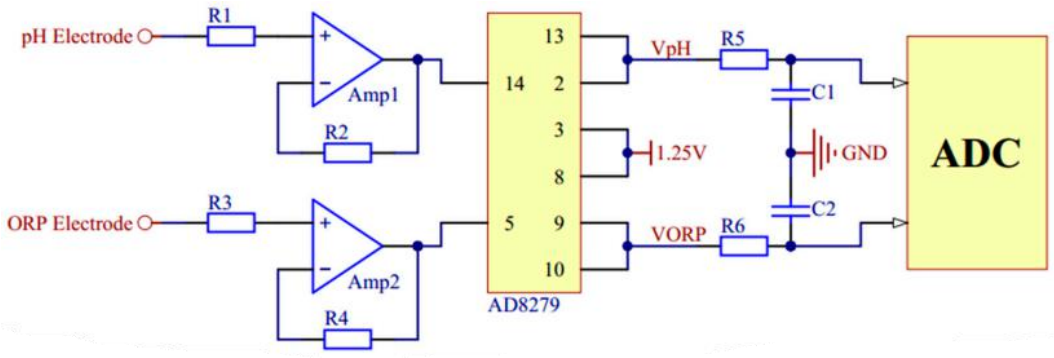

Figure 4. The signal conditioning circuit of pH and oxidation-reduction potential (ORP).

For temperature measurement, the Wheatstone bridge is used to convert the change of resistance value to voltage change. The voltage is amplified by using a single resistance amplifier AD8226 (Analog Devices, Norwood, MA, USA). The signal conditioning circuit of temperature is shown in Figure 5.

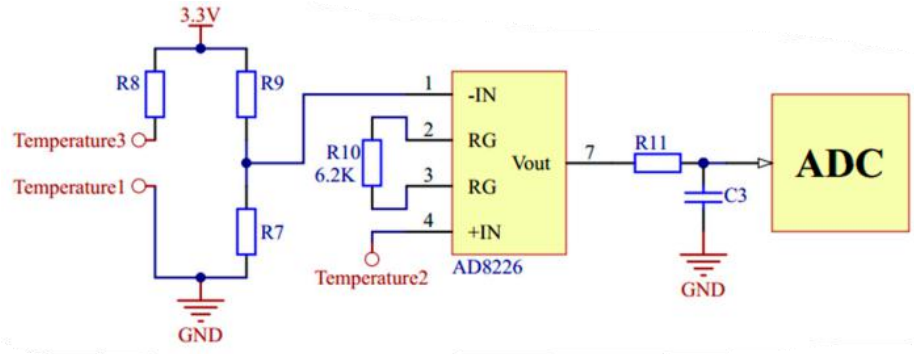

Figure 5. The signal conditioning circuit of temperature.

In the measurements of conductivity and copper irons, voltage excitation of specific frequency and amplitude is needed. A pulse width modulation circuit and a digital-to-analog converter (DAC) chip AD5662 (Analog Devices, Norwood, MA, USA) are used respectively to generate bipolar square wave and variable pulse voltage. The signal conditioning circuits of conductivity and copper irons are shown in Figure 6 and Figure 7.

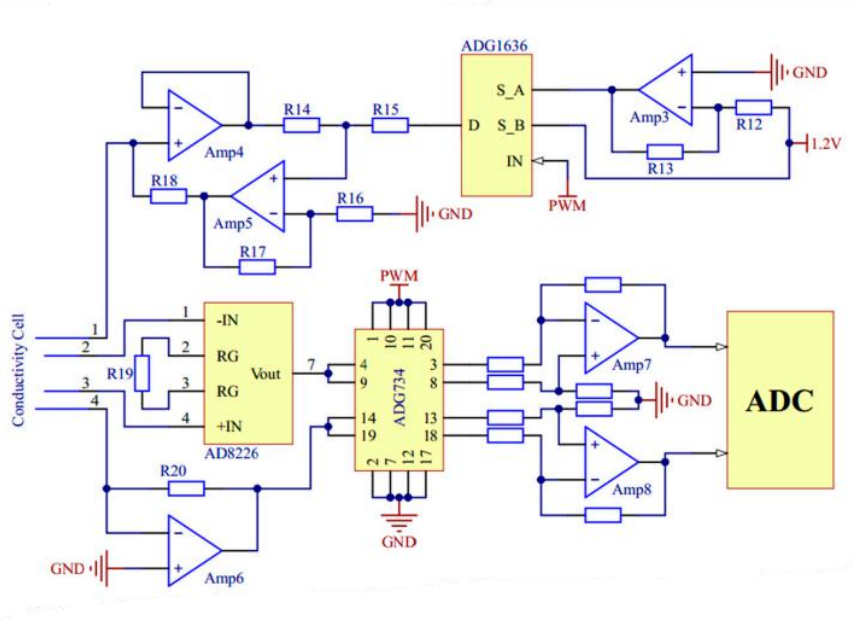

Figure 6. The signal conditioning circuit of conductivity.

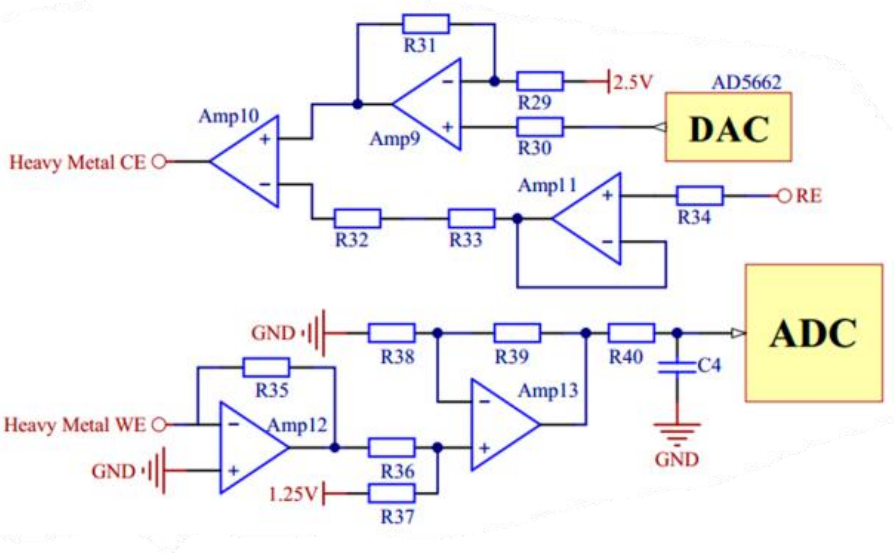

Figure 7. The signal conditioning circuit of copper irons.

Besides, the whole system also has a complete power management module to provide a stable and continuous power supply for all hardware components. The external power supply source is a lithium battery with a capacity of 1000 mA·h. Different precise voltages of ±3.3 V, 1.25 V, and 2.5 V are obtained through a series of low dropout regulator chips. The circuit boards of the portable detection system are shown in Figure 8. According to the functions in Figure 3, all the chips and devices are placed on a control board and a detection board.

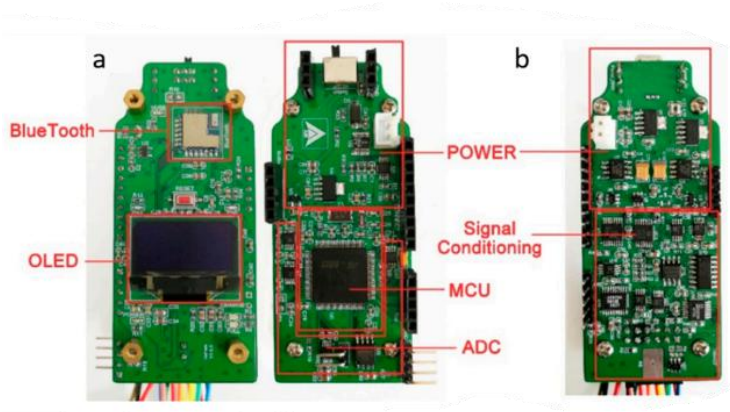

Figure 8. The circuit boards of the portable detection system: (a) Control board with both sides; (b) Detection board with the top side.

2.3. Software System

The embedded software program of the main controller was written in C language based on the Keil software integrated development environment. It mainly realizes the functions of hardware driver management, detection function selection, data calculation, and communication. A simple application (APP) was developed on the software Android Studio in Java language. The flowchart of the whole software system including embedded software and APP software program is shown in Figure 9a. A simple user interface (UI) and the background control instruction sending with data stream receiving of the APP [28] on the smartphone are shown in Figure 9b.

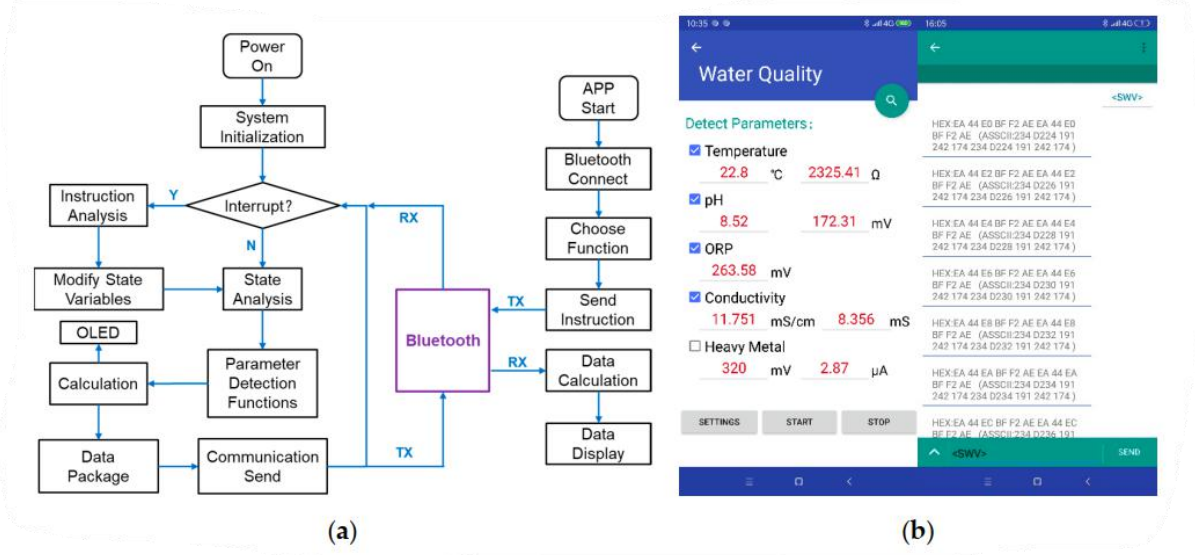

Figure 9. The software system: (a) Flowchart of the embedded software and application (APP) software; (b) A simple UI and the background data of the APP.

In the program, the detection of each parameter is encapsulated into each function. There are time interrupts and serial port interrupts in the MCU. In the interrupt service program, the instructions received from the serial port Bluetooth will be analyzed. The instructions are transmitted as char strings. On the mobile side, the instructions are sent by checkbox or text input. The instructions have a fixed format and a set of contents, which must be enclosed in angle brackets. Different contents of the instructions have different function commands. C language can analyze char strings easily and choose the needed program functions for multi-parameter detection. The detection data is also transmitted by the serial port. The data strings are encoded in ASCII. In this paper, through the serial port, a large amount of experimental data is sent to the computer besides the mobile phone. For the convenience of drawing the resulting diagram, the software Origin (Version 9.6.5, OriginLab, Northampton, MA, USA) is used on the computer.

For the OCP detection of voltage such as pH and ORP, we need to read the data in ADC chip, and then calculate the value of physical quantity. For temperature detection, the design of the hardware has already used the Wheatstone bridge to convert the resistance into voltage. The program reads the ADC and calculates it. According to the relationship between platinum thermal resistance and temperature in Equation (7), the temperature measurement can be obtained after the calibration process. In this paper, a 10 kHz bipolar square wave is used to measure the conductivity, which can eliminate the influence of the capacitance between electrodes [12]. Using the pulse width modulation function of the MCU, a 10 kHz unipolar square wave can be generated, and then the required bipolar excitation is obtained by the voltage inverter in the hardware circuit. The program controls reading ADC values while the square wave is applied. The measured conductivity value is obtained by voltage-ampere conversion and Ohm's law calculation. According to the calibrated electrode constant, the conductivity can be computed.

Common electrochemical methods for heavy metal ions detection are differential pulse voltammetry, linear sweep voltammetry and square wave voltammetry (SWV) [30,31]. Among them, SWV has higher sensitivity, wider linear range and low

detection limit according to the report [31]. In our study, SWV is used in the detection of copper ions. By analyzing the position and height of the dissolution peak in the voltage-current diagram, the concentration of copper ions is obtained [30]. In the software program, the value of pulse voltage is changed in each fixed interruption period, and the average values of the top and bottom of a single periodic pulse are taken as the data points in the volt-ampere curve. Similar to SWV, the function of the CV process is added to the software. The CV is mainly used to profile the electrochemical characteristics of the microelectrodes [4,23,31].

3. Results and Discussion

According to the aforementioned principles and equations (1,4–7), we carried out calibration experiments of the 5 parameters (pH, temperature, ORP, conductivity, and Cu^{2+}) using our portable detection system and chip. Except for the temperature calibration, all other experiments were performed at room temperature. The sensor chip was washed with deionized water between each measurement and dried in the flowing air. A photograph of the actual measurement is shown in Figure 10.

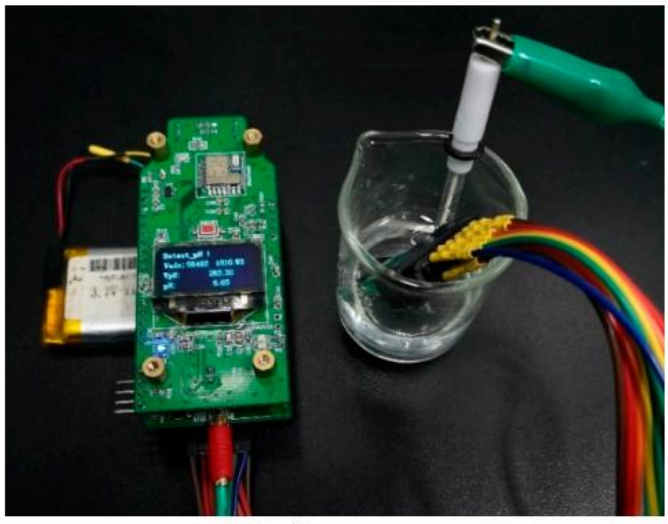

Figure 10. A photograph of the actual measurement.

3.1. pH and Temperature Calibration Measurements

Six standard solutions were prepared for pH measurement in the range of 4–11. The standard solutions consisted of 0.2M NaOH in different volumes added to the Britton Robinson buffer [12]. To ensure the correct configuration of the standard solutions, a pH meter (PHS-3C, INESA Scientific Instrument, Shanghai, China) with a glass electrode (E-201-9, Ruosull Technology, Shanghai, China) was used to measure the pH. The results were used as the x-axis data of the calibration curve. The calibration measurement started with the minimum standard solution (pH = 4.01) and increased. The time for the system to stabilize in each solution was within 30 s. Three repeated tests from 4.01 to 10.87 were carried out on our portable detection system. The calibration curve results are shown in Figure 11. The sensor shows a super-Nernst response of pH and has a sensitivity of −57.34 mV/pH, which is close to the theoretical value −59.14 mV/pH in Equation (4). The previously reported sensitivity −62.88 mV/pH of this kind of sensor was detected by an electrochemical workstation of GAMRY Reference 600 [12]. The result shows that our portable detection system has satisfactory detection capabilities. In the calibration curve, the span is calculated as 10.87−4.01=6.86. The maximum absolute error of pH measurement is 0.07 when pH = 9.18. The accuracy is computed as 0.07/6.86=1.02%.

Temperature measurements were carried out using a water bath heater (HH-1, Kewei Yongxing Instrument, Beijing, China) to steady the temperature and measured every 10 °C in the range of 10–70 °C for three times. The heated and measured solutions were fresh ice-water mixtures. We used an external metal cylindrical thermometer (Pt100, Sanxing Temperature Meter, Dongyang, China) as the standard rather than the set temperature of the heater, which could avoid control errors of the heater. The calibration curve is shown in Figure 12. The three-wire orthogonal Pt thermal resistor sensor has a temperature response capacity of 5.95 Ω/°C. For unknown solutions to be detected, using the portable system to measure the resistance of the RTD, the program can calculate the temperature by the equation in the calibration curve and display it on the OLED screen. In Figure 12, the maximum absolute error is 2.4 °C when the temperature is 59.1 °C. So the accuracy of temperature measurement is 2.4/(69.1−9.2) = 4.01%.

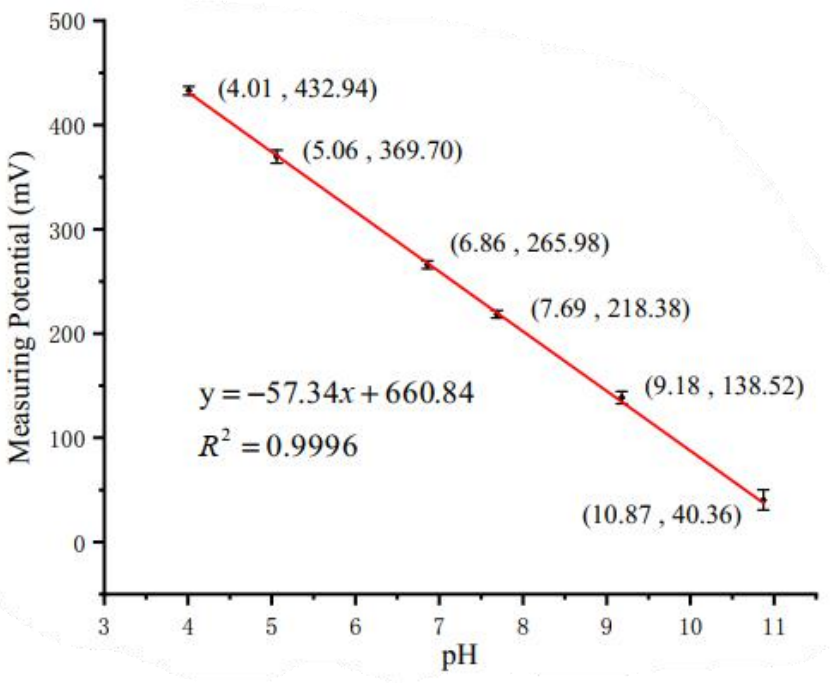

Figure 11. Calibration curve of pH sensor.

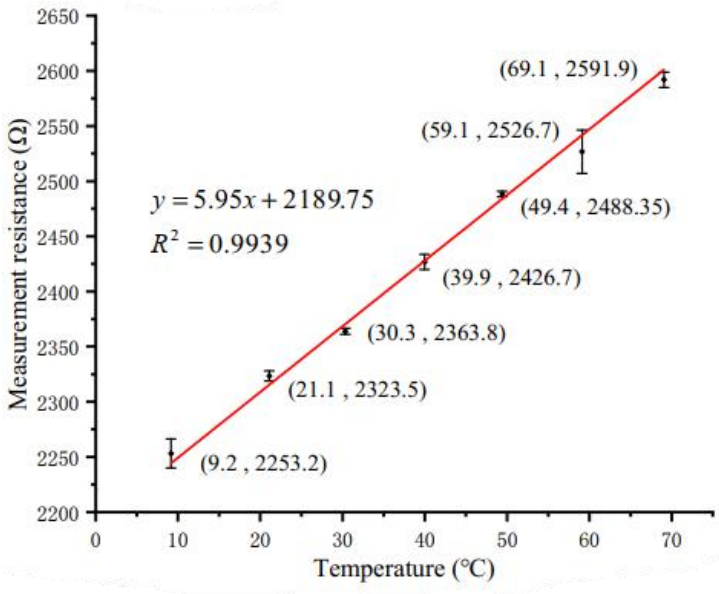

Figure 12. Calibration curve of temperature sensor.

3.2. ORP and Conductivity Calibration Measurements

Two standard solutions of 86 mV (quinhydrone solution with pH = 7) and 263 mV (quinhydrone solution with pH = 4) were used for ORP measurements. The RE was the Ag/AgCl glass electrode. The average values obtained by three measurements are 88.66 mV and 258.74 mV respectively as shown in Figure 13. The relative error

in the detection of the ORP sensor is less than 3%, which shows good precision and repeatability. Commercial ORP instruments typically use one-point calibration as standardization [32,33]. The standard solution can be a Light's solution (476 mV) or a ZoBell's solution (229 mV) [32]

A bipolar square wave at 10 kHz frequency was selected to excite the four-electrode ring conductivity sensor in our detection system. The sensor was calibrated with 7 standard solutions in the range of 1–22 mS/cm. These standard solutions were pure NaCl solutions with different mass percentage concentrations of 0.05, 0.10, 0.25, 0.50, 0.75, 1.00 and 1.24, respectively. At constant temperature, the fixed mass fraction solution has fixed conductivity [34]. A commercial portable conductivity meter (8306, AZ Instrument, Taichung, China) was used to measure the conductivity of these standard solutions at room temperature. The calibration curve of conductivity detection is shown in Figure 14. The electrode constant of the conductivity sensor is calculated as $1/0.706=1.416\ cm^{-1}$ from the three sets of volt-ampere characteristic data obtained by the portable meter. The experimental result shows that the four-electrode conductivity sensor has good linearity and sensitivity. When measuring unknown solutions, we first use the system to measure conductance and temperature values. Then the point of the conductance is substituted into the calibration curve in the detection program, and the conductivity of the solution is calculated using Equation (6). The measuring range of conductivity is 1.015–21.607 mS/cm. The maximum absolute error is 0.730 mS/cm, which includes calculation errors. The accuracy is computed as $0.730/(21.607-1.015)=3.55\%$.

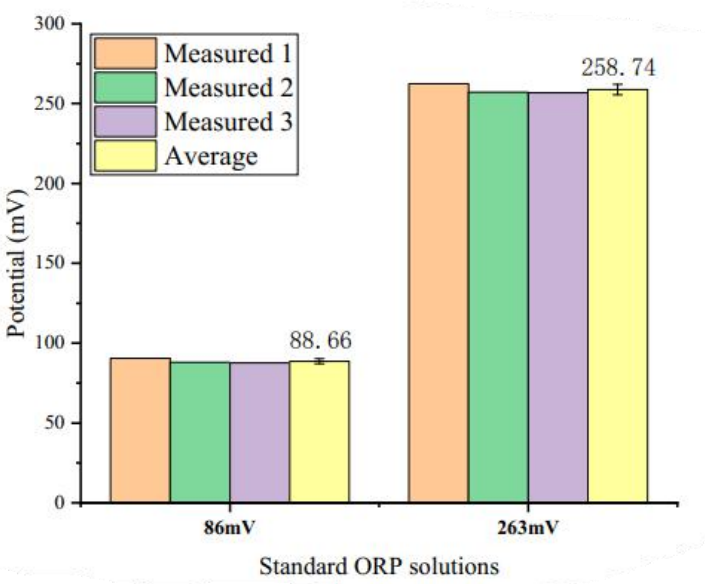

Figure 13. ORP detection result.

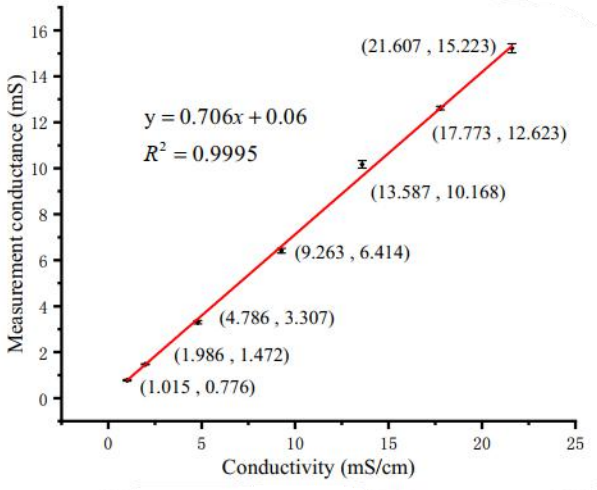

Figure 14. Calibration curve of conductivity sensor.

3.3. Copper Icons Measurement

In order to test the feasibility of the system for the detection of heavy metal ions in water, copper ions were chosen as the typical ions. The buffer solution was HAC-NaHAC solution with pH = 4.5. Four standard solutions with different copper ions concentrations (0.0, 0.2, 0.4, 0.6 mg/L) were used as the calibration solutions. To improve the detection sensitivity, a film of AuNPs was electrodeposited on the surface of the interdigital working electrode. The deposition was set at the potential −0.2 V in 2 mM HAuCl4 solution for 300 s. Figure 15 shows the CV characteristic curves of the interdigital electrodes in H2SO4 and K3[Fe(CN)6] solutions after deposition.

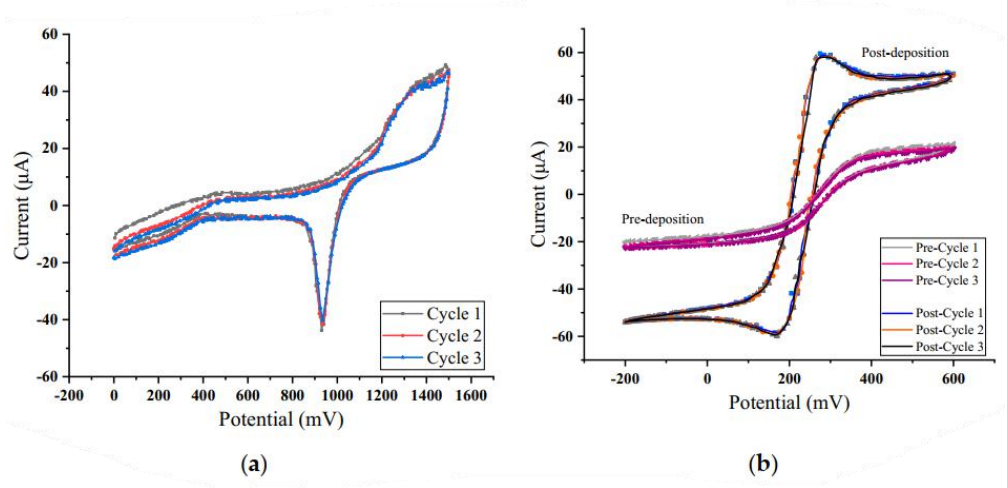

Figure 15. Cyclic voltammetry (CV) characteristic curves in: (a) H2SO4; (b) K3[Fe(CN)6].

As can be seen from Figure 15b above, the deposition of AuNPs can improve the redox characteristics of the interdigital electrodes. SWV scanning tests were carried out in copper ion solutions with different concentrations. The parameters of SWV are shown in Table 1.

Table 1. Square wave voltammetry (SWV) parameters setting.

Accumulation Time	Accumulation Potential	Step	Frequency	Initial Voltage	Final Voltage	Pulse Height
300 s	−600 mV	2 mV	25 Hz	−100 mV	800 mV	25 mV

The response curves of the sensor system to different concentrations of copper ion solutions are shown in Figure 16, in which only the current response ranging from 0–600 mV is shown. The order from bottom to top is 0.0, 0.2, 0.4, 0.6 mg/L. The peak potential of copper ion dissolution is 280 mV when the working electrode is a platinum interdigital electrode modified with AuNPs. The average value of each concentration is taken as the final peak current value at least three times after detection. The relationship between concentration and peak current is recorded and linear fitting is made as shown in Figure 17. The linearity for fitting a straight line is 0.9981.

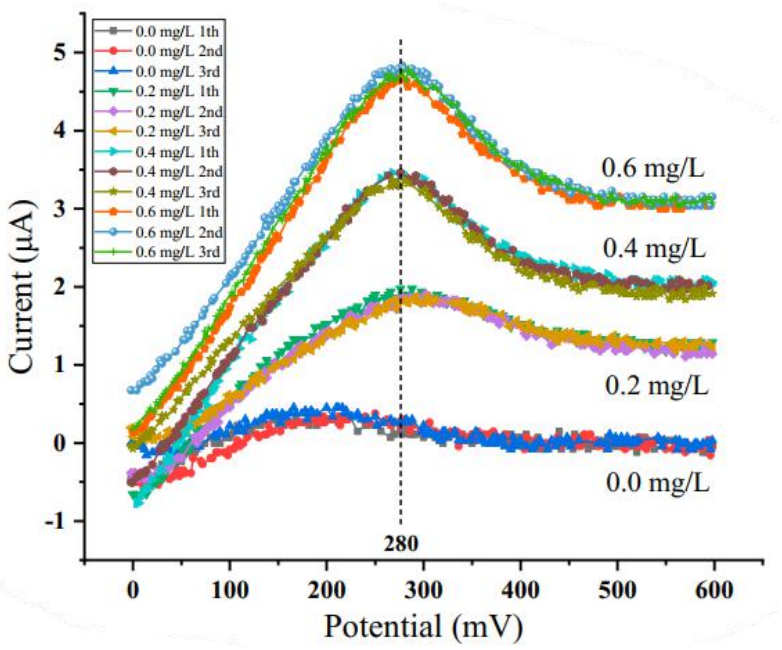

Figure 16. Cu2+ concentration-response curve.

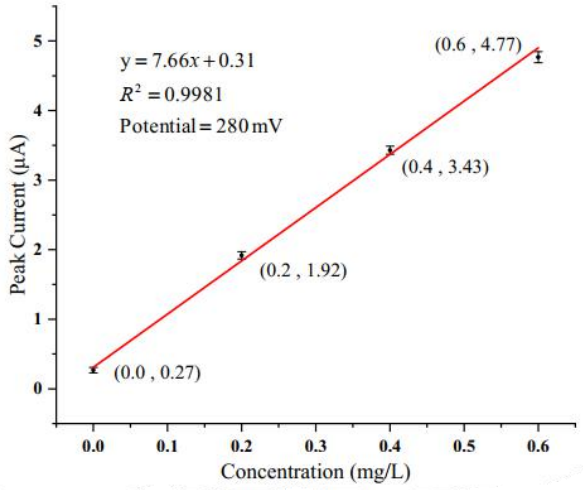

Figure 17. Cu2+ concentration-current fitting line.

The standard GB/T 5750-2006 [26] defines the detection limit as Equation (8).

$$D_L = 2\sqrt{2}t_f S_{wb} \tag{8}$$

where tf is the value of t at a significance level of 0.05 and degrees of freedom f. The f is obtained by subtracting one from the number of repeated detections. For three repeated measurements, the f is 2. In the statistical table, t2 is 2.92. Swb is the standard deviation of the blank sample. In this experiment of Cu2+, the standard deviation measured in the concentration of

0.0 mg/L is 0.04. According to Figure 17 and Equation (8), the detection limit of $\boldsymbol{Cu^{2+}}$ concentration is computed as 2.33 μg/L.

4. Conclusions

In this paper, a multi-parameter integrated sensor chip fabricated by MEMS technology is further studied, on which five different sensors are distributed, and its portable system for water quality detection is developed. Calibration experiments for all sensors were performed using the portable system. The pH sensor electrode fabricated by electrodepositing RuOx sensing material on the surface of the Pt electrode has a sensitivity of −57.34 mV/pH. The measuring range is 4.01–10.87 pH and the system presents an accuracy of 1.02%. ORP is directly detected by the Pt microelectrode and the relative error is less than 3%. The Pt thermistor with a three-wire orthogonal structure has a temperature response of 5.95 Ω/°C. In the measuring range of 9.2–69.1 °C, the accuracy of temperature is calculated as 4.01%. In the detection of conductivity solution in the range of 1–22 mS/cm, the sensor has an electrode constant of 1.416 cm−1 and the linearity is 0.9995, which shows an excellent linear detection performance of the sensor and the precise control of detection abilities. As to the detection of copper ions, AuNPs were deposited on the working electrode to improve the performance of the sensor. The peak current of the sensor shows a good linearity to the concentration of Cu2+ in the range of 0–0.6 mg/L. The detection limit of Cu2+ concentration is 2.33 μg/L. The experimental results show that this multi-parameter sensor chip and its portable system have the potential for on-site detection of various water quality parameters.

References

[1] Banna, M.H.; Imran, S.; Francisque, A.; Najjaran, H.; Sadiq, R.; Rodriguez, M.; Hoorfar, M. Online drinking water quality monitoring: Review on available and emerging technologies. *Crit. Rev. Environ. Sci. Technol.* 2014, *44*, 1370–1421. [Google Scholar] [CrossRef]

[2] Qin, Y.; Alam, A.U.; Pan, S.; Howlader, M.M.R.; Ghosh, R.; Hu, N.-X.; Jin, H.; Dong, S.; Chen, C.-H.; Deen, M.J. Integrated water quality monitoring system with pH, free chlorine, and temperature sensors. Sens. Actuators B Chem. 2018, 255, 781–790. [Google Scholar] [CrossRef]

[3] Chowdury, M.S.U.; Emran, T.B.; Ghosh, S.; Pathak, A.; Alam, M.M.; Absar, N.; Andersson, K.; Hossain, M.S. IoT based real-time river water quality monitoring system. Procedia Comput. Sci. 2019, 155, 161–168. [Google Scholar] [CrossRef]

[4] Zhou, B.; Bian, C.; Tong, J.; Xia, S. Fabrication of a miniature multi-parameter sensor chip for water quality assessment. Sensors 2017, 17, 157. [Google Scholar] [CrossRef] [PubMed]

[5] Martínez-Máñez, R.; Soto, J.; García-Breijo, E.; Gil, L.; Ibáñez, J.; Gadea, E. A multisensor in thick-film technology for water quality control. Sens. Actuators A Phys. 2005, 120, 589–595. [Google Scholar] [CrossRef]

[6] Qin, Y.; Alam, A.U.; Howlader, M.M.R.; Hu, N.-X.; Deen, M.J. Inkjet printing of a highly loaded palladium ink for integrated, low-cost pH sensors. Adv. Funct. Mater. 2016, 26, 4923–4933. [Google Scholar] [CrossRef]

[7] Banna, M.H.; Najjaran, H.; Sadiq, R.; Imran, S.A.; Rodriguez, M.J.; Hoorfar, M. Miniaturized water quality monitoring pH and conductivity sensors. Sens. Actuators B Chem. 2014, 193, 434–441. [Google Scholar] [CrossRef]

[8] Rotake, D.; Darji, A.D. Heavy metal ion detection in water using MEMS based sensor. Mater. Today Proc. 2018, 5, 1530–1536. [Google Scholar] [CrossRef]

[9] Jin, H.; Qin, Y.; Pan, S.; Alam, A.U.; Dong, S.; Ghosh, R.; Deen, M.J. Open-source low-cost wireless potentiometric instrument for pH determination experiments. J. Chem. Educ. 2018, 95, 326–330. [Google Scholar] [CrossRef]

[10] Giménez-Gómez, P.; Escudé-Pujol, R.; Jiménez-Jorquera, C.; Gutiérrez-Capitán, M. Multisensor portable meter for environmental applications. IEEE Sens. J. 2015, 15, 6517–6523. [Google Scholar] [CrossRef]

[11] Kruse, P. Review on water quality sensors. J. Phys. D Appl. Phys. 2018, 51, 203002. [Google Scholar] [CrossRef]

[12] Wang, J.; Bian, C.; Li, Y.; Sun, J.; Tong, J.; Xia, S. A multi-parameter integrated chip system for water quality detection. Int. J. Mod. Phys. B 2019, 33, 1950041. [Google Scholar] [CrossRef]

[13] Lin, W.-C.; Brondum, K.; Monroe, C.W.; Burns, M.A. Multifunctional water sensors for pH, ORP, and conductivity using only microfabricated platinum electrodes. Sensors 2017, 17, 1655. [Google Scholar] [CrossRef] [PubMed]

[14] Lee, W.H.; Lee, J.-H.; Choi, W.-H.; Hosni, A.A.; Papautsky, I.; Bishop, P.L. Needle-type environmental microsensors: Design, construction and uses of microelectrodes and multi-analyte MEMS sensor arrays. Meas. Sci. Technol. 2011, 22, 042001. [Google Scholar] [CrossRef]

[15] Qi, X.; Qian, J.; Chen, T.; Lu, D.; Chen, B. Electrochemical determination of Cu (II) ions based on Ag/Pd alloy for water quality early warning. Int. J. Electrochem. Sci. 2017, 12, 5511–5520. [Google Scholar] [CrossRef]

[16] Ghate, S.; Chaphekar, S.B. Plagiochasma appendiculatumas a biotest for water quality assessment. Environ. Pollut. 2000, 108, 173–181. [Google Scholar] [CrossRef]

[17] Campanella, L.; Cubadda, F.; Sammartino, M.P.; Saoncella, A. An algal biosensor for the monitoring of water toxicity in estuarine environments. Water Res. 2000, 35, 69–76. [Google Scholar] [CrossRef]

[18] Al-Yousuf, M.H.; El-Shahawi, M.S.; Al-Ghais, S.M. Trace metals in liver, skin and muscle of Lethrinus lentjan fish species in relation to body length and sex. Sci. Total Environ. 2000, 256, 87–94. [Google Scholar] [CrossRef]

[19] Lam, K.L.; Ko, P.W.; Wong, J.K.-Y.; Chan, K.M. Metal toxicity and metallothionein gene expression studies in common carp and tilapia. *Mar. Environ. Res.* 1998, *46*, 563–566. [Google Scholar] [CrossRef]

[20] Iyengar, G.V.; Nair, P.P. Global outlook on nutrition and the environment: Meeting the challenges of the next millennium. Sci. Total Environ. 2000, 249, 331–346. [Google Scholar] [CrossRef]

[21] Gómez-Ariza, J.L.; Sánchez-Rodas, D.; Giráldez, I.; Morales, E. A comparison between ICP-MS and AFS detection for arsenic speciation in environmental samples. Talanta 2000, 51, 257–268. [Google Scholar] [CrossRef]

基于微机电系统的多参数集成芯片和它的便携式水质检测系统

摘要

作为一种保护水资源的重要方法，水质检测有巨大的社会和经济效益。由微机电系统发展而来的水质检测传感器具有低功耗、小尺寸和低灵敏度的优点。本文深入研究了一种多参数水质检测集成传感器芯片，并开发了一种使用这款芯片的便携式检测系统。我们选取了温度，PH 值，氧化还原电位（ORP），电导率和铜离子浓度（Cu^{2+}）为典型水质参数，并使用了这款便携式检测系统在标准溶液中进行了传感器标定实验。传感器的 PH 检测灵敏度为-57.34mV/pH，温度响应灵敏度为 5.95Ω/℃。氧化还原电位由芯片上的铂微电极直接检测，相对误差小于 3%。该传感器的电极常数为 1.416cm^{-1}，电导率检测线性度为 0.9995。微电极上有纳米金沉积，Cu^{2+}的检测峰出现在 280 mV，传感器与Cu^{2+}浓度在 0～0.6 mg/L 范围内呈良好的线性关系。Cu^{2+}浓度的检出限为 2.33 $\mu g/L$。经过测量和计算，该便携式系统的精度在 4%的范围之内。这款配有基于微机电系统的集成芯片的多参数水质检测系统在快速检测领域展现了巨大的潜力。

一、前言

水污染已经吸引了全世界许多人的关注。水资源保护可以从检测水样中的理化指标的水质检测开始。通过水样检测可以获知水资源的污染状况并为后续的治理决策提供重要参考。由于缺乏迅速且有效的检测和治理措施，大规模的水污染事件仍然时常发生。在过去的三十年里，越来越多的研究聚焦于水质检测，专门的监管机构和组织颁布了大量指南和质量标准。传统的水质检测需要将水样带回实验室，这会消耗大量时间。随着计算机和通信技术的发展，水质检测仪器的发展趋势是低功耗，微型化，易操作，高精度和稳定性。

许多参数都可以被用来表征水质，包括 PH 值，浑浊度，游离氯，溶解氧，电导率，温度，氧化还原电位，重金属等等。仅检测单一参数不足以判断水质。然而，由于传感器探头的更换、调节和维护的复杂性，在现阶段对水中所有参数进行监测是不现实的。多参数，综合和同步检测是当前研究的热点。微传感器的产生和发展让多参数综合检测成为现实。这些集成传感器芯片的制造采用了先进成熟的厚膜技术、喷墨打印技术、微机电系统技术等工艺。远程便携水质检测常使用物联网技术，微机技术，以及 WiFi 和蓝牙等无线通信技术。

对于水质来说，温度是测定许多水质理化参数的重要因素，它可以直接影响 pH、电导率等监测项目的测量结果。除了玻璃液体温度计和双金属温度计外，热敏电阻也是常用的。其中，以铂为原料加工而成的电阻测温仪(RTD)因其稳定性好、精度高而被广泛使用。作为溶液酸碱度的量度，pH 值可以反映水质是被酸性物质污染还是碱性物质污染，并反映污染程度，这对人体健康非常重要。对于多参数集成传感器芯片及其便携系统来说，传统的 pH 玻璃电极并不是合适的选择。在以往的研究中，金属氧化物电极表现出良好的能斯特响应，其中 RuOx 具有低污染，易于制备和良好的耐化学性等特点。电导率是水质的电学和物理特性之一，反映了水中电解质的含量，是衡量水纯度的重要指标。ORP 监测最早出现在氯氧化能力的研究中，它的值与水质的消毒效率有关。目前，ORP 检测已被多项国际和国家卫生标准所认可。ORP 值作为饮用水标准，考虑了水中多种化学元素，便于用电子仪器显示水质。根据美国环境保护署(EPA)的规定，饮用水的 ORP

应接近 250 mV。ORP 是一个电化学参数，其电极的原理很清晰。测量它的直接方法是检测它对参照电极(RE)的电位。

重金属离子污染已成为严重的环境问题。在水生生态系统中，重金属离子改变了植物运动器官的精细结构，抑制了植物的光合作用和呼吸作用，改变了核酸的组成，影响了细胞体积。动物体内过量的重金属会导致酶失活和细胞毒性，进而影响基因表达，损伤神经组织和重要的免疫器官。传统的重金属离子检测方法包括但不限于原子荧光光谱法、电感耦合等离子体法、原子吸收光谱法、紫外-可见分光光度法和电化学检测等。电化学检测原理简单，仅用三电极系统即可实现。三电极系统由工作电极(WE)、对电极(CE)和参照电极 RE 组成。通过使用不同的材料对工作电极进行改造，可以实现对特定离子的识别，提高检测性能。例如，采用金纳米粒子改造的微电极(AuNPs)在检测铜、铅、锌离子方面表现出良好的分析性能。

本文进一步研究了一种多参数水质检测集成芯片。关于该集成芯片的温度、pH 和电导率传感器的设计、制作和测试结果已经发布，本文作了一些补充。本次研究重点是改进在该集成传感器芯片上对 ORP 和铜离子(Cu^{2+})的检测，并设计开发了上述 5 个参数的便携式检测系统。该多参数集成芯片采用和电化学改性技术制备，并制备了检测 ORP 电位的铂膜电极。铜铁检测传感器采用叉指电极结构，表面沉积 AuNPs 膜以提高检测能力。在我们的便携式检测系统中，采用了 STM32F407VGT6 芯片作为单片机，使用 0.96 英寸的有机发光二极管(OLED)屏幕显示数据，并在单片机的串口上连接蓝牙芯片，将数据传输到计算机或其他移动设备上，显示数据和波形。本项目旨在开发一种基于多参数集成传感器芯片的便携式水质检测系统，可用于检测水标准中的温度、pH、电导率、ORP 和铜离子等参数。在标准中，饮用水常温下的 pH 值应在 6.5~8.5 之间。一般天然水的电导率小于 1.5 mS/cm，而含无机盐的水可达 10mS/cm。水中铜离子的浓度应小于 1mg/L。本课题所提出的微机电系统传感器芯片及其便携式系统的实验结果表明，该系统在小型化、精度、线性度和灵敏度方面都取得了令人满意的效果。整个系统对实际水样的便携、快速、准确的测量具有很大的潜力。

二、材料和方法

2.1 多参数集成传感器芯片

考虑到铂具有良好的电气和温度特性，我们选择铂作为多传感器集成芯片。我们采用 4 英寸硅片加工技术和吉恩的微机电系统技术来制作为芯片每一部分的结构简化的制作过程如图 1 所示。在使用之前，硅片在浓缩的 H_2SO_4/H_2O_2 混合物以及去离子水中在 2000 $^{\circ}C$ 中连续蒸煮 20 分钟。之后，将硅片依次放入丙酮，酒精，去离子水中进行超声波清洗。由于硅具有导电性，因此有必要对硅表面进行氧化处理以实现绝缘。由热氧化形成的 SiO2 层厚度为 600-900nm。（图 1 步骤 1）然后使用氧等离子体对 SiO2 层表面进行清洗。我们使用光刻法使所需的传感器形状图案出现在硅片上。将金属钛和铂经氧等离子体清洗后，通过磁控溅射技术将其溅射到硅片表面传感器的位置上。（图 1 步骤 3）钛作为粘结金属，用于增强铂与基片的附着力。多余的金属和光刻胶用丙酮去除。重复上述步骤得到一层金属银，以供将来使用。（图 1 步骤 3）。之后仍通过光刻技术在传感器电极金属层形成一层光刻胶绝缘层。随后，将硅片切成一批 8mm×10mm 的单个芯片。多参数水质传感器集成芯片如图 2 所示。最后每块芯片都通过金丝球焊接到 PCB 板上。

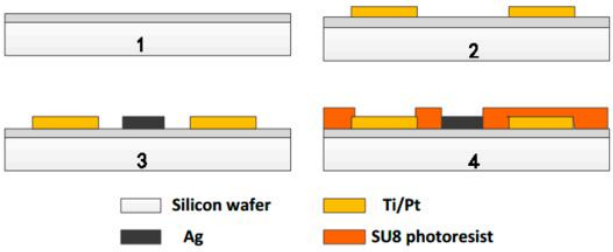

Figure 1. Fabrication process of the integrated microchip.

硅片　　钛/铂

银　　SU8 光刻胶

图 1：集成微芯片的制作过程

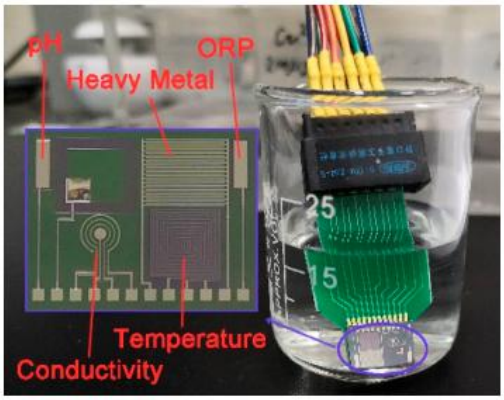

Figure 2. Multi-parameter integrated chip.

酸碱度 重金属 氧化还原电位 电导率 温度

图 2： 多参数集成芯片

pH 电极和 ORP 电极的形状都是矩形，大小为 500 μm ×2000 μm 。这两个参数的基本原理相似，都是基于（1）式所述的能斯特方程中的电位法。

$$E = E_0 + \frac{RT}{nF}\ln\frac{A_{ox}}{A_{red}} \quad (1)$$

其中 E 是金属电极表面产生的电势。E0 是标准电极电位（ mV ）。R 为理想气体常数（8.314 $J \bullet mol^{-1}K^{-1}$ ）。F 是法拉第常数。符号 n 表示反应中电子转移的次数。 A_{ox} 代表氧化物质的活性， A_{red} 为还原性物质的活性。显然，我们需要测量的电位 E 受到热力学温度 T（K）的影响。ORP 传感器的测量电极是惰性铂电极，它可以起到传递电子的作用，并且不参与反应。因此，铂可以通过检测铂微电极相对于 Ag/ $AgCl$ 参比电极的电位作为毫伏的单一电压来直接测量。铂测量单元用于检测 ORP 的变化，而参照电极提供稳定的比较信号。

RuO_x 对溶液的 pH 值敏感。在 RuCl3 溶液中，通过循环伏安法在铂微电极表面沉积一层 RuO_x 层后，RuO_x /Pt 电极与 Ag/ $AgCl$ 参比电极结合成为 pH 传感器。简化后的 RuO_x 诱导机理可由式（2）描述。 RuO_x 的能斯特方程简化为式（3）。

$$R_u{}^{IV}O_2 + e^- + H^+ = R_u{}^{III}O(OH) \quad (2)$$

$$E_{p^H} = E_0 - \frac{RT}{F} ln \frac{c(R_u{}^{III})}{c(R_u{}^{IV}) \cdot c(H^+)} \quad (3)$$

c(Ru^{III})和 c(Ru^{IV})分别代表 Ru(III)和 Ru(IV)的活性。在固态时，它们几乎相等。C(H^+)为H^+的浓度，它的负对数为 pH，在 25 $^{\circ}C$时，其近似为（4）式。

$$E_{p^H} = E_0 + 0.05914 \times \lg c(H^+) \quad (4)$$

这意味着理论斜率为-59.14mV/pH。与 ORP 一样，pH 传感电极测量开路电位。

电导率传感器设计为四电极形。4 电极导电性传感器的优点在于，内电极上流过的电流在测量时可以忽略不计。电导率与电阻率成反比。它是一个电物理量，其与电压、电流的关系如式（5）所示。

$$S = k \cdot G = k \cdot I/U \quad (5)$$

其中，S 为电导率(mS/cm)，k 为电极常数(cm^{-1})，G 为电导(mS)，I 为电流(μA)，U 为电压(mV)。检测方法是对传感器施加交流刺激，并测量其上流过的电压和电流。根据实验测量的电压，电流和电极常数，可以计算出水质的电导率。此外，电导率受温度的影响如式（6）所示。

$$S_t = S_{18}[\alpha(t - 18) + 1] \quad (6)$$

S_t是 t ◦C 时的电导率(mS/cm)，S_{18}表示 18 ◦C 时的电导率(mS/cm)，符号 α 是温度系数($^{\circ}C^{-1}$)。

如前所述，电阻测温仪（RTD）被广泛用于测量温度。其电阻-温度特性可表示为式（7）。

$$R_t = R_0 \cdot [1 + \beta(t - t_0)] \quad (7)$$

这里 R_t 代表着在 t $^{\circ}C$ 时的电阻值（Ω），R_0 代表着在 t_0 ℃时的电阻值（Ω）。β 是材料的温度系数（$^{\circ}C^{-1}$）。测量电阻值的方法很简单。本研究中的温度传感器是正交结构的铂微带，连接采用三端连接方式。

在检测铜离子时，我们建立了一种电化学三电极系统，设计了两排叉指电极，分别为 WE 和 CE。每一排的电极由 15 个手指电极（3500μm×50μm）构成，指状组合间距为 50μm。通过循环伏安法在 2mM 的 $HAuCl_4$ 溶液中的 WE 电极表面上沉积了一层 $AuNPs$ 薄膜。沉积电位为-0.2V，沉积时间为 300s。在这种 3 电极系统中，采用 Ag/ $AgCl$ 电极作为参比电极。

2.2 硬件系统

检测系统由如上所述的集成传感器芯片、控制模块、人机交互模块、模数转换（A/D）和信号处理电路组成。检测系统的硬件框图如图 3 所示。

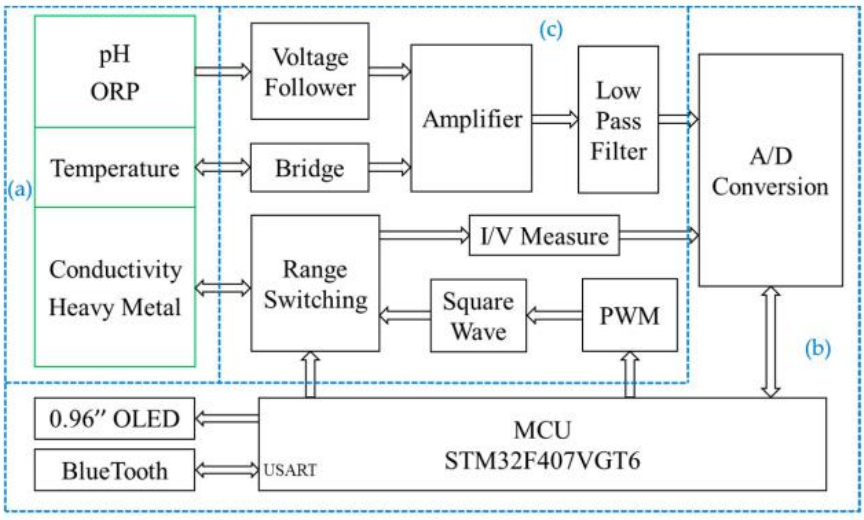

酸碱度　　电压跟随器　放大器　　低通滤波器　模/数转换

氧化还原电位　桥接器　　电流/电压测量

温度　　波段开关　　方波发生器　　脉冲宽度调制

电导率

重金属

0.96 OLED　　微控制单元 STM32F407VGT6

蓝牙

图 3:硬件系统框图：（a）集成传感器芯片（b）控制模块，人机交互模块和 A/D 转换（控制板）；（c）信号处理电路（检测板）

控制模块采用 STM32F407VGT6 芯片（意法半导体公司，日内瓦，瑞士）作为微控制单元，它包含由外部晶振、调试接口、复位电路等组成的最小系统。人机交互模块由一块 0.96 英寸的 OLED 屏幕、蓝牙单元（BLE103 芯片，文恒科技，上海，中国）以及 USART 串行通信端口组成。采用 OLED 屏幕显示实时数据，提示系统运行状态，直接显示测量结果。通过蓝牙通信，将便携式水质检测系统与智能手机连接，实现功能控制、数据传输和分析。为了在本地存储大量的数据，我们使用 USART 端口将数据传输到计算机。数据处理和结果曲线绘制使用 Origin 软件（版本 9.6.5，*OriginLab*,北安普顿,马萨诸塞州，美国）。测量时使用了低功率模数转换器（ADC）芯片 AD7790（模拟设备，诺伍德,马萨诸塞州，美国）. 在 2.5V 的参考电压下，最小的测量值为 0.0763mV。当 pH 传感器作用于 -59.14mV/pH 时，我们能检测到的 pH 最小理论变化为 0.0763/59.14=0.0013pH。在检测系统中，仅保留两位小数，即可达到 0.01pH 的分辨率。

信号处理电路主要包括滤波器，运算放大器和信号产生电路。测量 pH 和 ORP 时，使用了 AD8279 芯片（模拟设备，诺伍德,马萨诸塞州，美国）来将上述两个参数的电压放大或降低两倍。然后再加上 1.25V 的补偿电压，从而得到 0-2.5V 的测量电压。考虑到阻抗匹配，采用了两个电压跟随器。pH 和 ORP 的信号处理电路如图 4 所示，它们的参考电极都通过一个电阻与 GND 零电位相连。

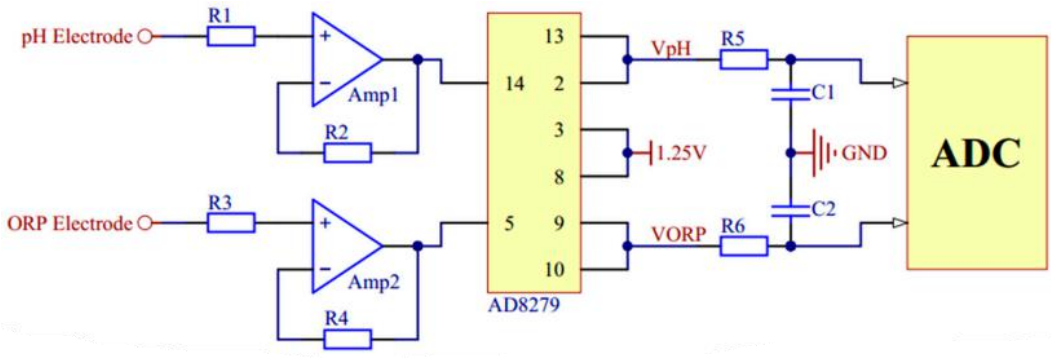

酸碱度电极　　模数转换器

氧化还原电极

图 4： pH 和氧化还原电位（ORP）的信号处理电路

在测量温度时，利用惠斯通电桥将电阻值的变化转化为电压的变化。使用单电阻放大器 AD8226（模拟设备，诺伍德，马萨诸塞州,美国）将电压放大。温度信号处理电路如图 5 所示。

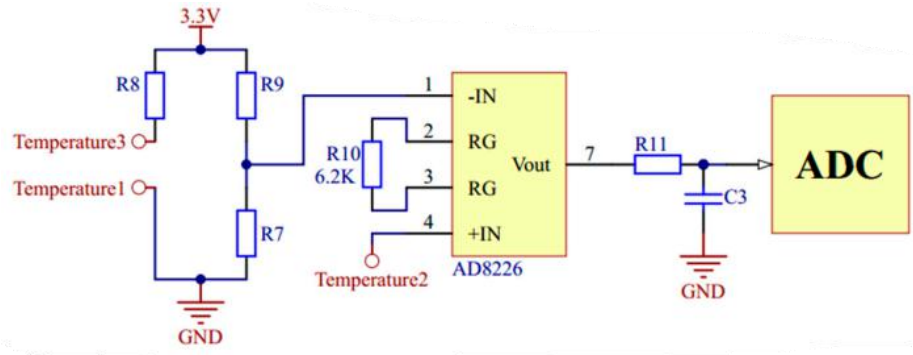

温度 1　温度 2　温度 3　模数转换器

图 5： 温度信号处理电路

测量电导率和铜离子时，需要特定频率和振幅的电压激励。采用脉宽调制电路和数模转换（DAC）芯片 AD5662（模拟设备，诺伍德，马萨诸塞州,美国）分别产生双极方波和可变脉冲电压。电导率和铜离子信号处理电路如图 6 和图 7 所示

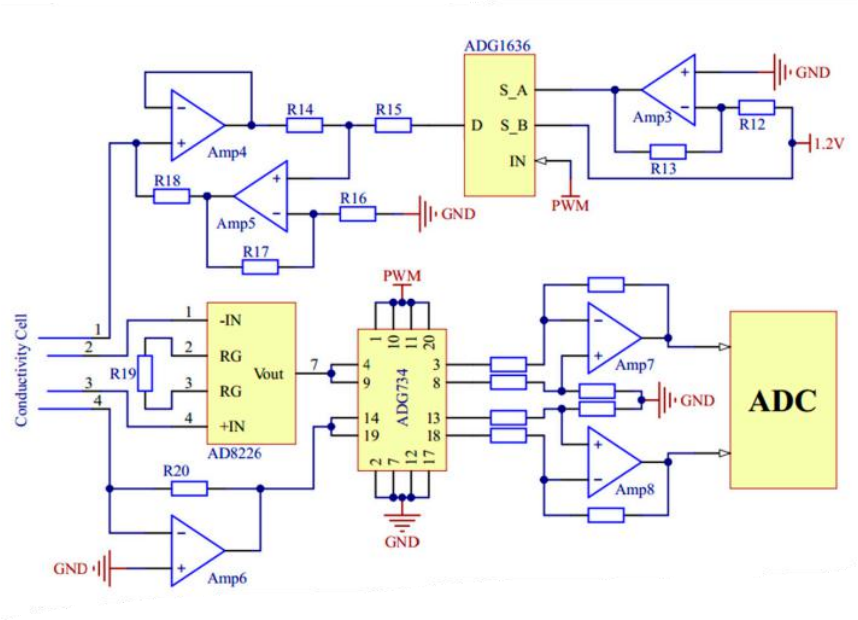

脉冲宽度调制

图 6： 电导率信号处理电路

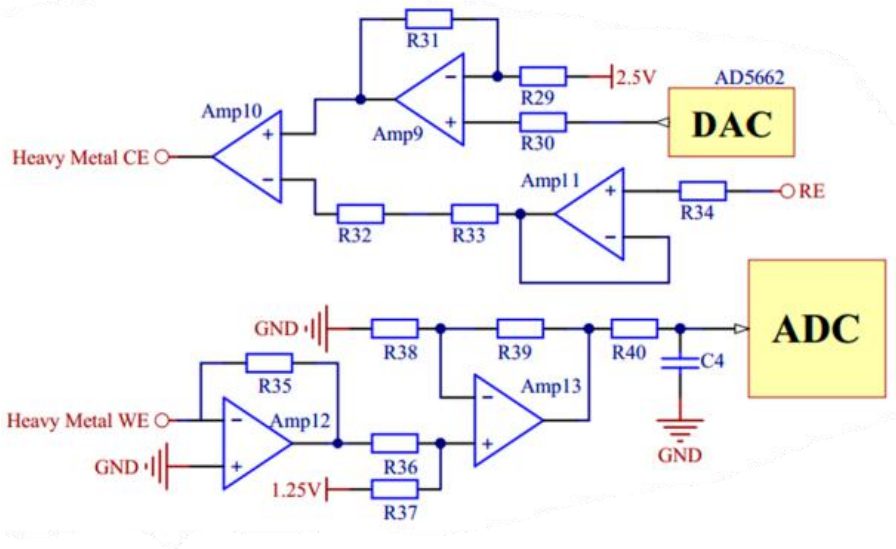

重金属对电极 参比电极 数模转换

重金属工作电极 模数转换

图 7： 铜离子信号处理电路

此外，整个系统还有一个完整的电源管理模块，为各硬件部件提供稳定、持续的电源供应。外部电源为 1000mA·h 的锂电池，通过一系列低压降稳压器芯片获得±3.3V、1.25V 和 2.5V 的不同精确电压。便携式检测系统的电路板如图 8

所示。根据图 3 的功能，将所有芯片和设备分别放置在一个控制板和一个检测板上。

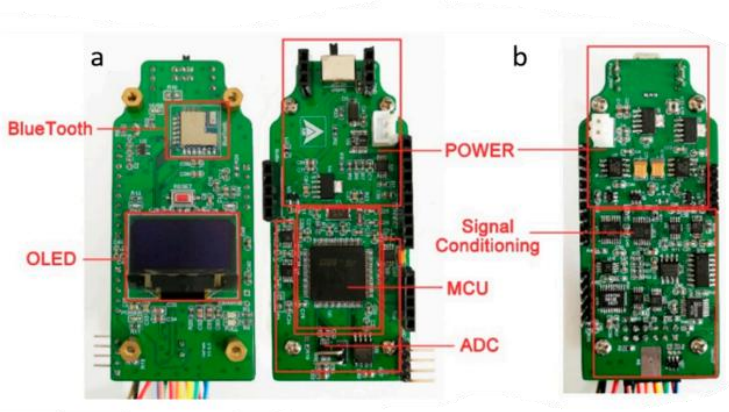

蓝牙 有机发光二极管 电源 信号处理 微控制单元 模数转换

图 8： （a）控制板的两侧 （b）检测板的顶部

2.3 软件系统

主控制器的嵌入式软件程序采用 C 语言编写，并基于 K*eil* 软件集成开发环境，它主要实现了硬件驱动管理，检测功能选择，数据计算和通信等功能。在 Android Studio 上用 Java 语言开发了一个简单的应用程序（APP），包括嵌入式软件和 APP 软件程序在内的整个软件系统流程图如图 9a 所示。图 9b 所示为手机上该 APP 的一个简单的用户界面(UI)以及后台控制指令发送时的数据流接收。

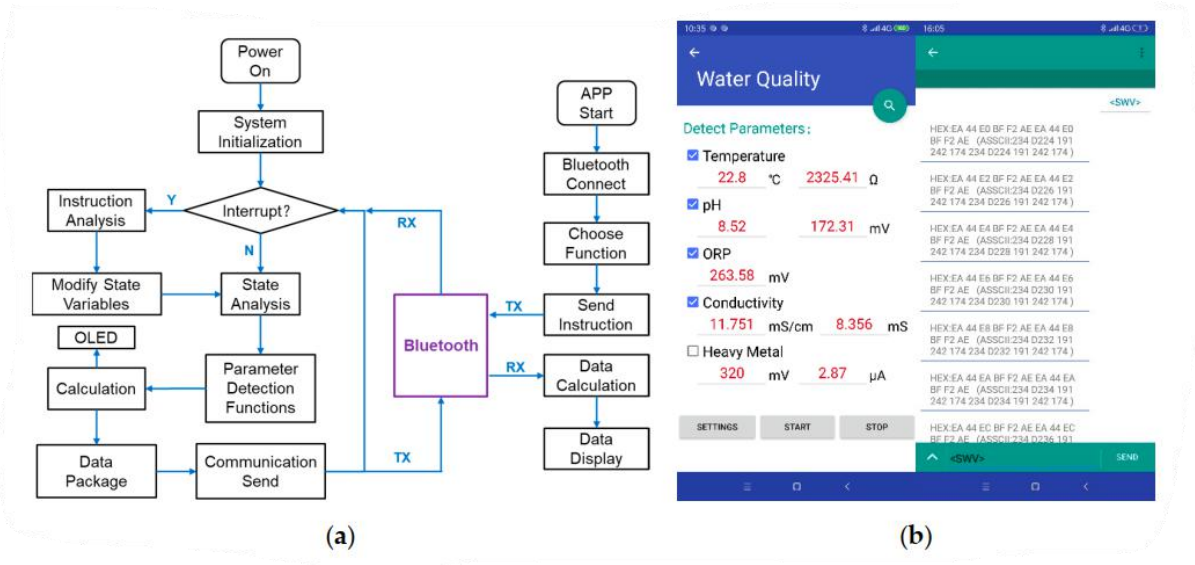
Power On
System Initialization
Interrupt?
Y
N
Instruction Analysis
Modify State Variables
State Analysis
OLED
Calculation
Parameter Detection Functions
Data Package
Communication Send
RX
TX
Bluetooth
TX
RX
APP Start
Bluetooth Connect
Choose Function
Send Instruction
Data Calculation
Data Display
Water Quality
Detect Parameters:
Temperature
22.8 ℃ 2325.41 Ω
pH
8.52 172.31 mV
ORP
263.58 mV
Conductivity
11.751 mS/cm 8.356 mS
Heavy Metal
320 mV 2.87 μA
SETTINGS
START
STOP
SEND
(a)
(b)

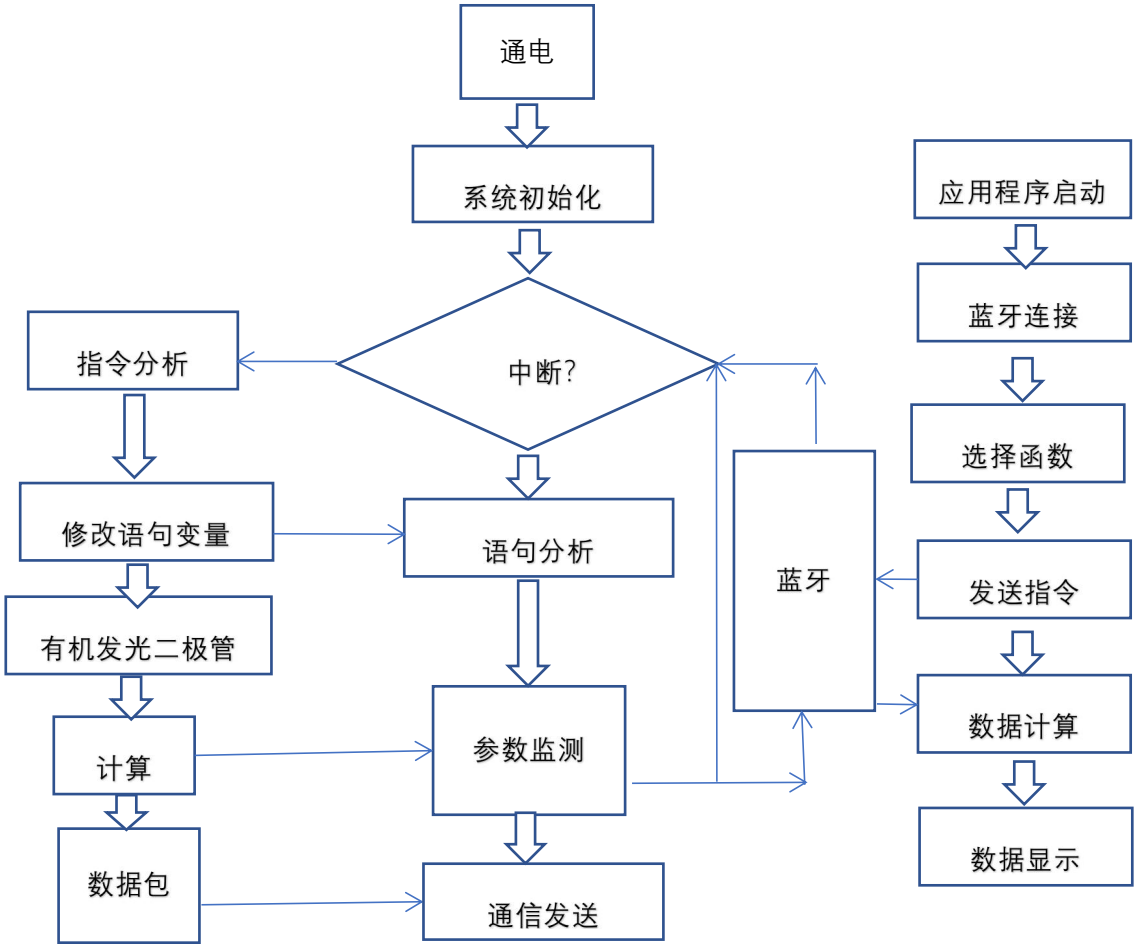
通电
系统初始化
中断?
指令分析
修改语句变量
有机发光二极管
计算
数据包
语句分析
参数监测
通信发送
蓝牙
应用程序启动
蓝牙连接
选择函数
发送指令
数据计算
数据显示

（a）

图 9 软件系统：(a)嵌入式软件及应用软件流程图；(b)一个简单的 UI 和 APP 的后台数据。

在程序中，每个参数的检测被封装到每个函数中。主控制单元（MCU）中存在时钟中断和串口中断。在中断服务程序中分析从串口蓝牙接收到的指令。指令以字符串的形式传输。在移动端，指令通过复选框或文本输入发送。指令有固定的格式和一组内容，这些内容必须通过尖括号括起来。指令的不同内容包含不同的功能命令。C 语言可以方便地分析字符串，选择所需的程序函数进行多参数检测。检测数据也通过串口传输。数据字符串使用 ASCII 编码。在本文中，通过串口将大量的实验数据发送到手机和电脑上。为了方便绘制结果图，在计算机上使用 Origin 软件（版本 9.6.5,*OriginLab*，北安普顿,马萨诸塞州，美国）。

在进行 PH 和 ORP 的开路电位检测时，需要读取 ADC 芯片中的数据，之后再计算物理量的值。在检测温度时，硬件电路的设计已经使用了惠斯通电桥以将电阻转化为电压，程序读取 ADC 的值并计算。根据式（7）中反应的铂热阻和温度的关系，标定过程结束后可以得到温度测量值。本文采用 10kHz 的双极性方波来测量电导率，可以消除极间电容的影响。使用脉宽调制 MCU 可以产生一个 10kHz 的单极方波，然后在硬件电路中通过电压反相器得到所需的双极电压。当施加方波之后，用程序控制读取，电阻率是通过电压-安培变换和欧姆定律计算得到的。根据标定的电极常量，可以计算出电导率。

常用的重金属离子电化学检测方法是微分脉冲伏安法、线性扫描伏安法和方波伏安法。报告显示，在这三者之中，方波伏安法具有更高的灵敏度，更宽的线性范围以及更低的检出限。在我们的研究中，方波伏安法用于检测铜离子。通过分析伏安图中溶液峰值的位置和高度，可以得到铜离子的浓度。在软件程序中，脉冲电压的值在每个固定的中断周期都会改变,并以单个周期脉冲顶部和底部的平均值作为伏安曲线上的数据点。与方波伏安法类似，循环伏安法的过程也被加入到软件中，它主要是用于表征微电极的电化学特性。

三、结果

根据前述的原理和等式（1,4-7），我们使用便携式检测系统和芯片进行了五个参数（酸碱度,温度，ORP,电导率，和Cu^{2+}）的标定实验。除了温度标定，其他实验都是在室温下进行的。传感器芯片在每两次测量之间用去离子水清洗，并在流动的空气中干燥。实际测量的照片显示在图 10 中。

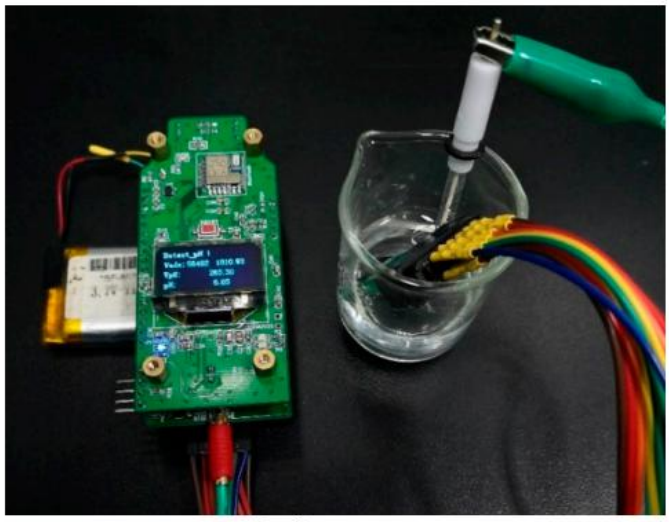

图 10： 一张实际测量的照片

3.1 酸碱度和温度标定测量

我们配制了 pH 范围在 4-11 之间的六种溶液用于 pH 测量。标准溶液为不同量的 0.2M *NaOH* 加入到 *Britton Robinson* 缓冲液中。为了确保标准溶液的正确配置，还使用了带有玻璃电极（E-201-9,若苏科技，中国，上海）的 pH 计（PHS-3C INESA 科学仪器，上海，中国）用于测量 pH,测量结果用作标定曲线的 x-轴数据。校准测量从最低标准溶液（pH=4.01）开始，pH 值逐渐增加，在每种溶液中检测系统都可以在 30s 之内稳定下来。我们在便携系统上进行了 4.01-10.87 之间的三次重复实验。校准曲线结果如图 11 所示。该传感器显示出对 pH 的超能响应，灵敏度为-57.34mV/pH，这与方程（4）中的理论值-59.14mV/pH 很接近。此前曾报道过的这种传感器的灵敏度为-62.88mV/pH 是通过 GAMRY Re*feren* 600 电化学工作站测量得到的。结果显示，我们的便携式检测系统具有良好的检测能力。

在标定曲线中，跨度为 10.87-4.01=6.86. pH=9.18 时，测量最大绝对误差为 0.07，计算出精度为 0.07/6.86=1.02%.

温度测量时使用水浴加热器（HH-1,科威永兴仪器，北京，中国）来稳定温度，并在 10-70◦C 范围内每 10◦C 测量三次。加热和测量的溶液是纯净的冰水混合物。我们使用的是外置金属圆柱形温度计(Pt100,中国东阳三兴温度计)，作为标准，而不是加热器的设定温度，这样可以避免加热器的控制误差。标定曲线如图 12 所示。三线正交铂热敏电阻传感器的温度响应能力为 5.95$\Omega/^{\circ}C$. 对于待测未知溶液，利用便携式系统测量 RTD 的电阻，程序可以根据标定曲线中的方程计算出温度，并显示在 OLED 屏幕上。在图 12 中，当温度为 59.1C 时最大绝对误差是 2.4$^{\circ}C$。因此温度测量的精度是 2.4/(69.1-9.2)=4.01%.

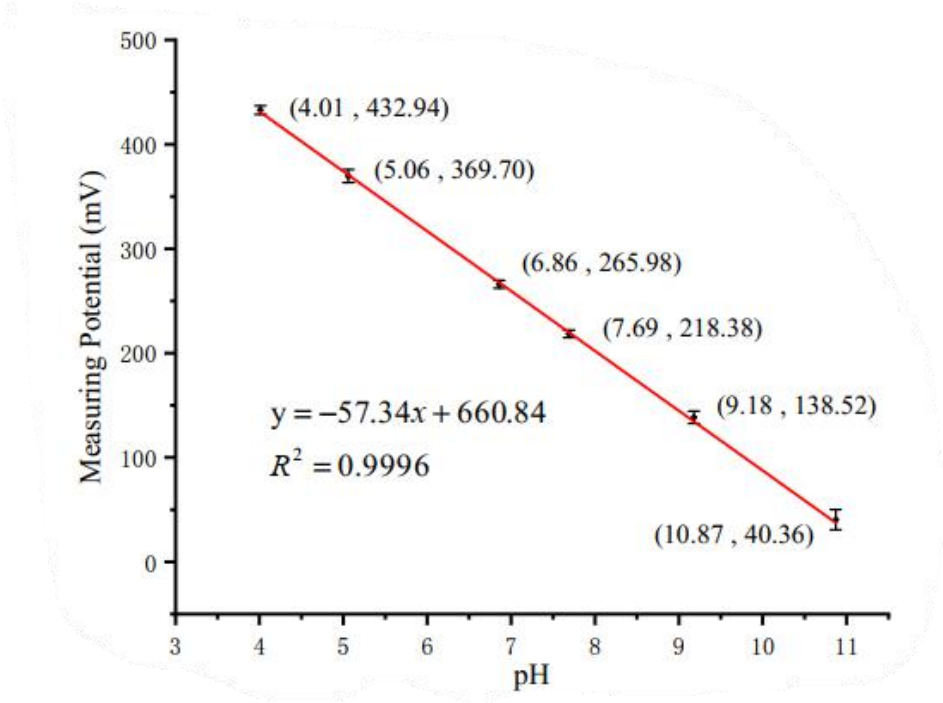

纵轴：测量电位　　横轴：酸碱度

图 11：　酸碱度传感器的测量曲线

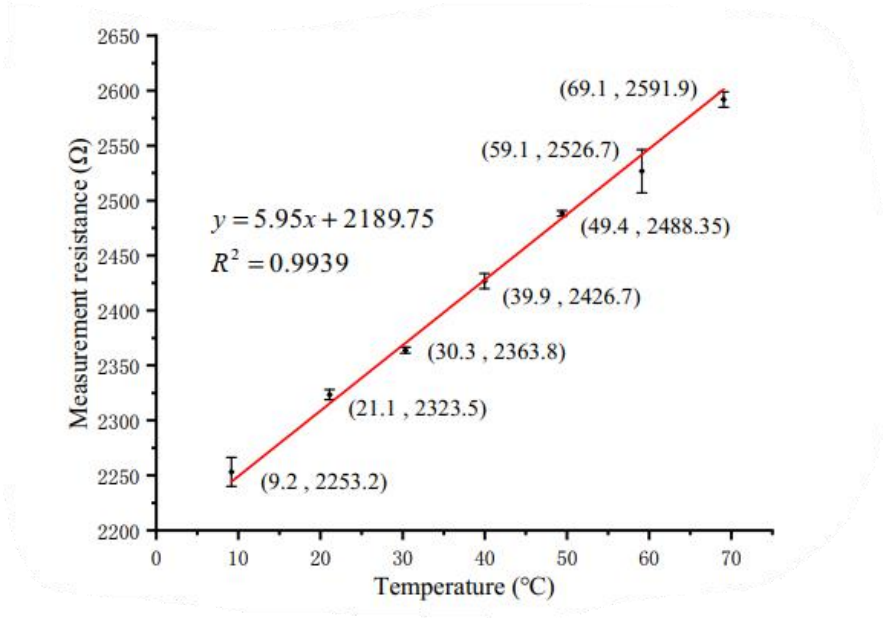

纵轴：测量阻抗　　横轴：温度

图 12：温度传感器的标定曲线

3.2 ORP 和电导率标定测量

测定 ORP 的标准溶液为 86mV 的（pH=7 的喹酮溶液）和 264mV(pH=4 的喹酮溶液)。参比电极为 Ag/ *AgCl* 玻璃电极。正如图 13 所示，由三次测量所得的两种溶液的 ORP 平均值分别是 88.66mV 和 258.74mV。ORP 传感器的检测相对误差小于 3%，具有良好的精度和可重复性。商用 ORP 仪器通常使用单点标定来进行标准化。标准溶液可以是赖特溶液(476mV)或佐贝尔溶液(229mV).

在本检测系统中，我们选择了频率为 10KHz 的双极方波来激励四电极环电导率传感器，传感器使用 7 种电导率的值在 1-22mS/cm 范围内的标准溶液进行校准。这些标准溶液是质量百分比浓度不同的纯 *NaCl* 溶液，分别为 0.05,0.10,0.25,0.50,0.75,1.00 和 1.24。在恒温条件下，固定质量分数溶液具有固定电导率。采用商用便携式电导率仪(8306,AZ Instrument，台中，中国)测定了这些标准溶液在室温下的电导率。电导率检测校准曲线如图 14 所示。由便携式测量仪测得的三组伏安特征数据计算所得的电导率传感器电极常数为 1/0.706=1.416 cm^{-1} . 实验结果显示四电极电导率传感器具有良好的线性度和灵

敏度。当测量未知溶液时，我们首先使用检测系统去测量电导率和温度值，之后检测程序会将这些电导率的测量点绘成校准曲线，并使用公式（6）计算出溶液的电导率值。电导率的测量范围是 1.015-21.607 mS/cm 。最大绝对误差是 0.730 是 mS/cm 包括计算误差，计算所得精度为 0.730/（21.607-1.015）=3.55%。

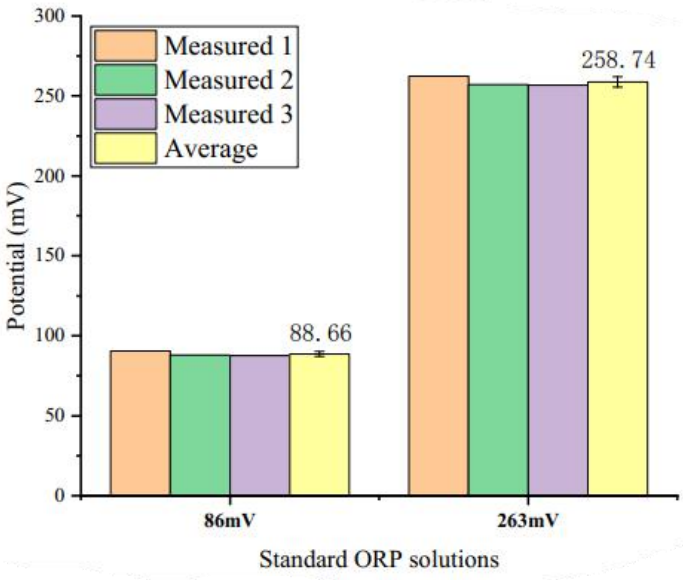

纵轴：电位　　横轴：标准氧化还原溶液

图 13：ORP 检测结果

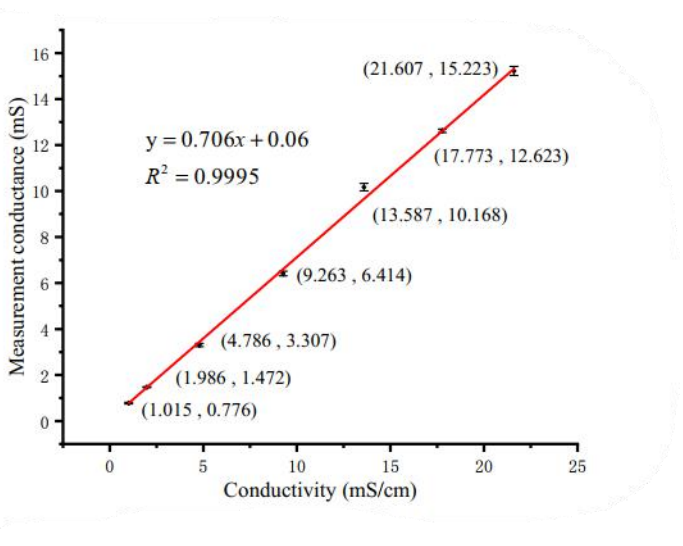

纵轴：测量阻抗　　横轴：电导

图 14：电导率传感器校准曲线

3.3 铜离子测量

为了验证该系统检测水中重金属离子的可行性，以铜离子作为典型离子。缓冲溶液为 pH=4.5 的 $HAC-NaNAC$ 溶液。以四种不同铜离子浓度（0.0，0.2，0.4,0.6mg/L）的标准溶液作为校准溶液。为提高检测灵敏度，在叉指电极表面电沉积一层 *AuNPs* 薄膜。在 2mMHAuCL4 溶液中，沉积电位设为-0.2V，持续时间为 300s。图 15 为 H_2SO_4 和 K3[Fe(CN)6]溶液在沉积之后的叉指电极的循环伏安法（CV）特征曲线。

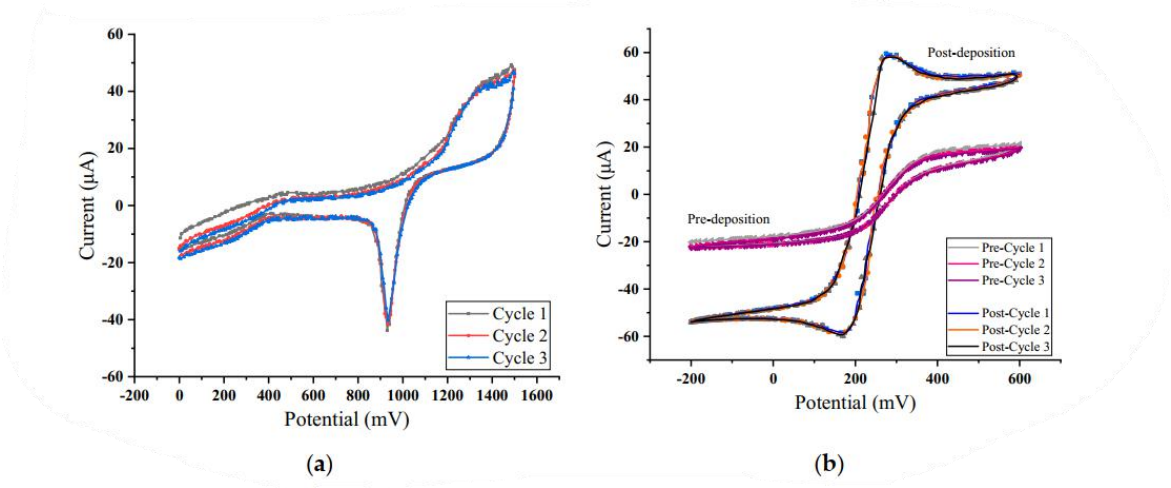

纵轴：电流　横轴：电势　　纵轴：电流　　横轴：电势

图 15：循环伏安法（CV）特征曲线：(a) H_2SO_4；(b) $K_3[Fe(CN)_6]$.

从上图 15b 可以看出，*AuNPs* 的沉积可以改善叉指电极的氧化还原特征。在不同浓度的铜离子溶液中进行了方波伏安法的扫描检测。方波伏安法的参数如下表 1 所示。

表 1　方波伏安法参数设置

Accumulation Time	Accumulation Potential	Step	Frequency	Initial Voltage	Final Voltage	Pulse Height
300 s	−600 mV	2 mV	25 Hz	−100 mV	800 mV	25 mV

累积时间　累积电势　步进　频率　初始电压　最终电压 脉冲高度

传感器系统对不同浓度的铜离子溶液的响应曲线如图 16 所示，途中仅显示了范围在 0-600mV 之间的电流响应。从下到上的顺序是 0.0，0.2，0.4，0.6mg/L。当工作电极是用 *AuNPs* 改造过后的铂叉指电极时铜离子溶液的峰值电势是 280mV。在至少经过三次检测之后，将平均值作为每种浓度溶液的最后峰值电流值。图 17 记录了浓度和峰值电流的关系并进行了线性拟合。拟合直线的线性度为 0.9981。

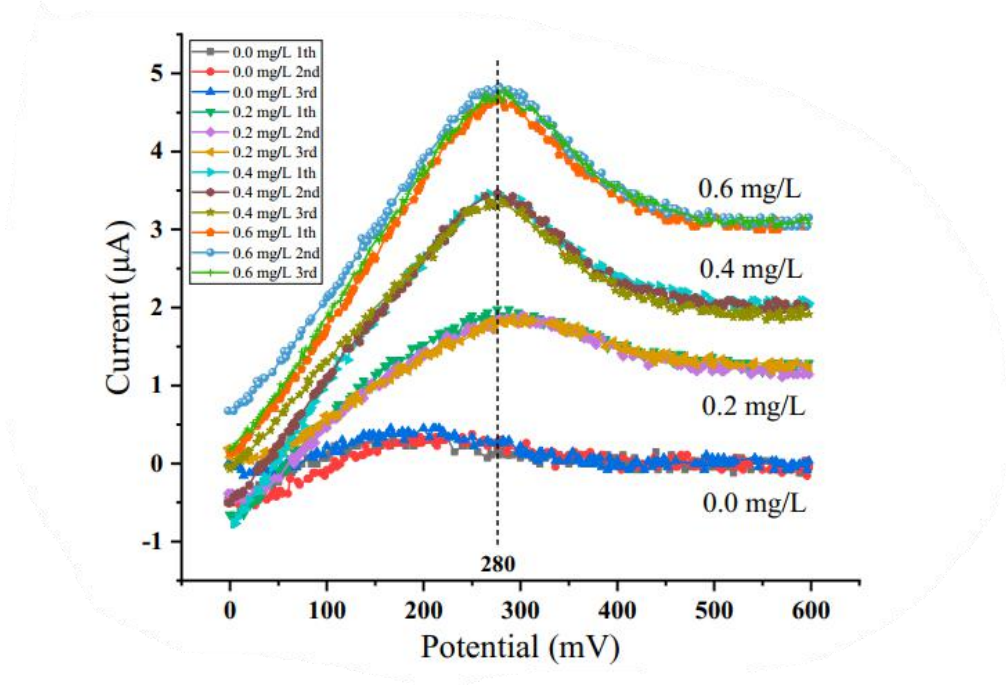

纵轴：电流　　横轴：电势

图 16：Cu^{2+} 浓度-响应曲线

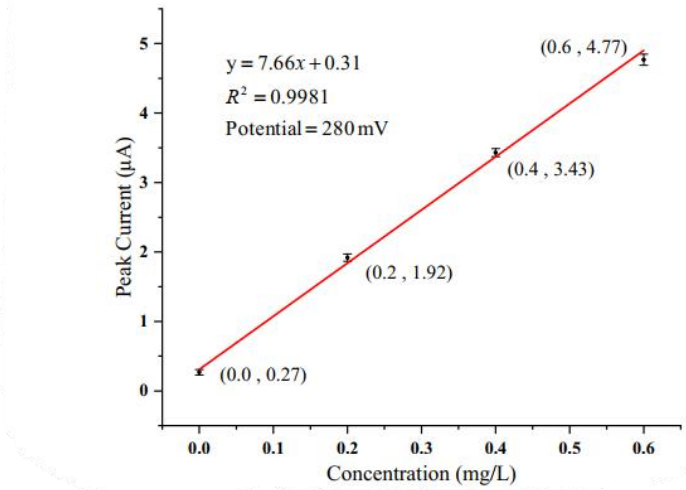

纵轴：峰值电流　　横轴：浓度

图 17：Cu^{2+}浓度-电流拟合直线

GB/T 5750-2006 标准将检出限定义为式（8）。

$$D_L = 2\sqrt{2}t_f S_{wb} \tag{8}$$

式中，显著性水平为 0.05 时的 t 值为t_f，自由度为 f，f 为重复检测次数减 1.当进行三次重复测量时，f 是 2.在统计表中，t 为 2.92。S_{wb}是空白样品的标准差。在本次S_{wb}实验中，浓度为 0.0mg/L 的溶液测得的标准差是 0.04。根据图 17 和式（8），计算出S_{wb}浓度的检出限为 2.33 $\mu g/L$。

四、总结

本文进一步研究了利用 MEMS 技术制作的多参数集成传感器芯片，在该芯片上分布 5 个不同的传感器，并开发了便携式水质检测系统。利用该便携系统对所有传感器进行了校准实验。在铂电极表面电沉积RuO_x传感材料制备的 pH 传感器电极的灵敏度为-57.34mV/pH，测量范围为 4.01-10.87pH,测量精度为为 1.02%。用铂微电极直接测量 ORP，相对误差小于 3%。三线正交结构的铂热敏电阻的温度响应是 5.95$\Omega/^{\circ}C$。在 9.2-69.1$^{\circ}C$的测量范围内，温度的精度计算为 4.01%。对 1-22mS/cm 范围内的电导率溶液的检测，该传感器的电极常数为 1.416cm^{-1}，线性度为 0.9995，表明该传感器具有优良的线性检测性能和精确的检测能力控制。在测量铜离子时，在工作电极上沉积 *AuNPs* 以提高传感器的性能。传感器峰值电流与Cu^{2+}浓度在 0～0.6mg/L 范围内呈良好的线性关系。Cu^{2+}的检出限为 2.33$\mu g/L$。实验结果表明，该多参数传感器芯片及其便携系统具有现场检测各种水质参数的潜力。

参考文献

1. 班纳，伊姆朗，弗朗西斯科，娜迦仁，罗德里戈，霍尔法，在线饮用水质量监测.对现有和新兴技术的回顾.环境科学与技术重要评论.2014,44,1370-1421.

2. 秦仪，阿莱姆，潘， 郝来德,戈什,胡,津,冬,陈,仃.酸碱度、游离氯、温度传感器的集成水质监测系统.2018,255,781-790

3. 周独瑞,埃姆朗,戈什,帕萨克,阿莱姆,阿巴沙,安德森,侯赛因,基于物联网的实时河流水质监测系统.2019-155,161-168

4. 周必,边超,童佳,水质评估微型多参数传感器芯片的构成.2017,17,157

5. 马丁内斯·马来兹,索托,加西亚·布内久,吉尔；伊巴内兹,加迪尔,一种用于水质控制的厚膜多传感器技术.2005,120,589-595

6. 秦·伊,阿莱姆,郝来德,胡,仃.用于集成、低成本酸碱度传感器的高负载钯油墨的喷墨打印.2016,26,4923-4933

7. 班纳,娜迦仁,萨迪克,伊姆朗,鲁迪格兹,霍尔法.微型水质监测酸碱度和电导率传感器.2014,193,434-441

8. 若泰克·迪,秦·伊,潘,阿莱姆,冬,戈什,仃.使用基于微机电系统的传感器进行水中重金属离子检测 2018,5,1530-1536

9. 金和,秦伊,潘,阿莱姆,冬,戈什,仃.用于 pH 测定实验的开源低成本无线电位仪.2015,15,6517-6523

10. 吉门内兹·戈每兹,艾斯苦德·普居尔,吉门内兹·月奎尔,古提内兹·卡皮坦,环境应用的多传感器便携式仪表.2018,15,6517-6523

11. 克鲁兹·皮；水质传感器回顾。2018,51,203002

12. 王吉,边超,李仪,孙洁,童佳,夏思,一种多参数水质检测集成芯片系统.2019,33,1950041

13. 王林,布荣多姆·肯,蒙若；崩丝,仅使用微型铂电极的酸碱度，氧化还原电位和电导率的多功能水传感器.2017,17,1655

14. 李伟含,李洁和,周伊,霍斯尼,帕波斯凯,比硕普. 针型环境微传感器：多电极和多组分微机电传感器阵列的设计、制造和使用。2011,22,042001

15. 齐西,钱季,陈天,卢冬,陈毕.水质预警中的基于银、钯合金的铜离子电化学测定.2017,12,5511-5520

16. 戈特,查皮卡尔,海尾斜沟水质评估的生物试验.2000,108,173-181
17. 卡佩拉,库巴达,萨玛提诺,索恩赛拉,一种用于检测河口环境水毒性的藻类生物传感器.2000,35,69-76
18. 阿尔·约瑟夫,沙哈伊,阿尔·加伊斯,黑腮蓝鳌鱼肝脏、皮肤、和肌肉中微量金属含量与体长和性别的关系.2000,256,87-94
19. 兰姆,科,王吉凯,陈凯蒙,鲤鱼和罗非鱼金属毒性及金属硫蛋白基因表达研究.1998,46,563-566
20. 艾杨格,奈尔,营养与环境的全球展望,应对未来一千年的挑战.2000,249,331-346
21. 戈麦斯·阿里萨，桑切斯·罗达斯，吉拉尔德兹，莫拉莱斯，电感耦合等离子体质谱与原子荧光谱谱仪检测环境样品中砷形态的比较.2000,51,257-268